NASA/TM—2006-214413

Aerodynamic Performance Measurements for a Forward Swept Low Noise Fan

E. Brian Fite
Glenn Research Center, Cleveland, Ohio

December 2006

NASA STI Program . . . in Profile

Since its founding, NASA has been dedicated to the advancement of aeronautics and space science. The NASA Scientific and Technical Information (STI) program plays a key part in helping NASA maintain this important role.

The NASA STI Program operates under the auspices of the Agency Chief Information Officer. It collects, organizes, provides for archiving, and disseminates NASA's STI. The NASA STI program provides access to the NASA Aeronautics and Space Database and its public interface, the NASA Technical Reports Server, thus providing one of the largest collections of aeronautical and space science STI in the world. Results are published in both non-NASA channels and by NASA in the NASA STI Report Series, which includes the following report types:

- TECHNICAL PUBLICATION. Reports of completed research or a major significant phase of research that present the results of NASA programs and include extensive data or theoretical analysis. Includes compilations of significant scientific and technical data and information deemed to be of continuing reference value. NASA counterpart of peer-reviewed formal professional papers but has less stringent limitations on manuscript length and extent of graphic presentations.

- TECHNICAL MEMORANDUM. Scientific and technical findings that are preliminary or of specialized interest, e.g., quick release reports, working papers, and bibliographies that contain minimal annotation. Does not contain extensive analysis.

- CONTRACTOR REPORT. Scientific and technical findings by NASA-sponsored contractors and grantees.

- CONFERENCE PUBLICATION. Collected papers from scientific and technical conferences, symposia, seminars, or other meetings sponsored or cosponsored by NASA.

- SPECIAL PUBLICATION. Scientific, technical, or historical information from NASA programs, projects, and missions, often concerned with subjects having substantial public interest.

- TECHNICAL TRANSLATION. English-language translations of foreign scientific and technical material pertinent to NASA's mission.

Specialized services also include creating custom thesauri, building customized databases, organizing and publishing research results.

For more information about the NASA STI program, see the following:

- Access the NASA STI program home page at *http://www.sti.nasa.gov*

- E-mail your question via the Internet to *help@sti.nasa.gov*

- Fax your question to the NASA STI Help Desk at 301–621–0134

- Telephone the NASA STI Help Desk at 301–621–0390

- Write to:
  NASA STI Help Desk
  NASA Center for AeroSpace Information
  7121 Standard Drive
  Hanover, MD 21076–1320

NASA/TM—2006-214413

Aerodynamic Performance Measurements for a Forward Swept Low Noise Fan

E. Brian Fite
Glenn Research Center, Cleveland, Ohio

National Aeronautics and
Space Administration

Glenn Research Center
Cleveland, Ohio 44135

December 2006

Acknowledgments

The design and fabrication of the majority of hardware was completed on NASA contract NASA3–27752 as part of the Advanced Subsonic Technology Project. Contributions of the project team including Joe Grady and Dennis Huff of NASA Glenn Research Center and Don Weir of Honeywell Engines and Systems were vital. The guidance and suggestions of Don Weir, Russ Repp, and Dave Gentile of Honeywell Engines and Systems are appreciated. Without the efforts of Tom Gyekenyesi, QSS Group, Inc., Al Linne, and Marty Krupar of NASA Glenn and the contributions of many machinists, fabricators, technicians, and mechanics, this test would not have been possible. Finally, the author wishes to gratefully acknowledge the ongoing assistance and suggestions from colleagues Bob Jeracki and Chris Hughes from NASA Glenn and John Gazzaniga of QSS Group, Inc.

Level of Review: This material has been technically reviewed by technical management.

Available from

NASA Center for Aerospace Information
7121 Standard Drive
Hanover, MD 21076–1320

National Technical Information Service
5285 Port Royal Road
Springfield, VA 22161

Available electronically at http://gltrs.grc.nasa.gov

Aerodynamic Performance Measurements for a Forward Swept Low Noise Fan

E. Brian Fite
National Aeronautics and Space Administration
Glenn Research Center
Cleveland, Ohio 44135

Summary

One of the many sources of noise present in a high tip speed turbofan jet engine is multiple pure tone noise (MPT's). When the fan tip speeds become supersonic, MPT's are generated through interaction of the rotor shock structure and the inlet duct. This particular type of noise is often present during take-off and landing conditions when the engine is at a part throttle operating condition and, if present, has a negative affect on community noise impact as well as certification of the engine for service with respect to noise requirements.

A fan stage was designed by Honeywell Engines and Systems, Inc. to reduce MPT's using a modern turbofan jet engine fan stage as the baseline. The new fan, called the Quiet High Speed Fan (QHSF), was tested and shown to reduce noise over the part speed region, which includes MPT's, as desired. The goal was to reduce fan noise while matching, or improving, the performance capability over the baseline fan with respect to fan pressure ratio, mass flow, efficiency, and operability margin. The QHSF shows improved performance in most respects relative to the baseline fan; however, a part-speed instability discovered during testing reduced the fan operating range below acceptable limits. The new fan stage had a design point (100 percent corrected speed) peak adiabatic efficiency of 85.9 percent compared to 83.3 percent for the baseline fan stage, a 2.6 percent improvement. The measured adiabatic efficiency on the fixed nozzle acoustic operating line showed the QHSF efficiency was 85.1 percent and the baseline fan 82.9 percent, a 2.2 percent improvement. The operating line pressure rise at design point rotational speed and mass flow was 1.764 and 1.755 for the QHSF and baseline fans, respectively. Weight flow at design point was 98.28 lbm/sec for the QHSF and 97.97 lbm/sec for the baseline fan. Unfortunately, the operability margins for the QHSF approached 0 percent at the part speed operating conditions near 75 percent speed. The baseline fan maintained sufficient margin throughout the operating range as expected. Based on the stage aerodynamic measurements, this concept shows promise for improved performance over current technology if the operability limitations can be solved.

Introduction

The National Aeronautics and Space Administration support many activities in advanced propulsion research and technology for commercial aircraft. Specifically, the NASA Glenn Research Center, as the center of excellence for air breathing turbomachinery, is involved in performance and emissions research for future aircraft. The recently completed Advanced Subsonic Technology program included specific aircraft noise reduction goals of 10 dB at each of the three aircraft measurement locations—approach, sideline, and takeoff. More specifically, the noise reduction goal for the engine was –6 dB at each of these measurement locations. The fan is a significant noise source in modern engines and therefore was one of the components targeted for study to meet these goals. A series of fans were built and tested to evaluate acoustic and aerodynamic performance. This report details the steady state performance measurements of one of these fans designated Quiet High Speed Fan (QHSF) and a baseline fan used for comparison. The QHSF was designed and built by Honeywell Engines and Systems of Phoenix, Arizona to study the effect of forward sweep as a potential noise reduction technique (refs. 1 and 2). A baseline fan was also supplied by Honeywell which is a scaled version of the fan used for the TFE731-60 engine. The QHSF was designed to have identical performance parameters as the baseline engine.

Test Hardware and Procedure

Background

For fans with tip speeds that are supersonic, one noise source is generated by the rotor-locked shock structure interacting with the inlet duct and radiating to the far-field (refs. 2 and 3). The spectrum associated with this noise source includes a tone for each fan blade and is called Multiple Pure Tone (MPT) noise. As a supplier of engines for business and regional aircraft applications, Honeywell Engines and Systems is familiar with propulsion systems that have high tip Mach numbers. These systems can benefit greatly through technology that will allow the management of MPT noise through novel design techniques and blade geometry tailoring.

The goal of this effort is to design a fan blade that reduces MPT noise using blade forward sweep while maintaining high efficiency and appropriate operability margins. The forward sweep is being used to control leading edge normal Mach number and contain the passage shock over the operating range of the fan. This concept was investigated previously and is described in reference 4.

Baseline Fan (Honeywell 731–60 fan)

The fan selected to serve as the baseline for this test was a scaled model of the TFE731-60 engine fan. This fan was selected as the baseline because it has MPT's present in the normal operating range of the engine and it is the product of a recent fan design process and therefore will provide a current generation baseline for which the benefits of the QHSF will be compared. The fan tip speed, along with other specific aerodynamic design parameters, is shown in table 1 and a picture of the fan is shown in figure 1. In this report and associated plot legends, the baseline fan is referred to as the "baseline" fan and "–60" fan.

TABLE 1.—FAN DESIGN PARAMETERS

Specific aerodynamic design parameters	
Fan aero design point, 100 percent fan corrected speed, 22 in. diameter	
Parameter, units	Value
Wcorr, lbm/sec	98.9
Wcorr/A, lbm/s/ft^2	42.7
Tip speed (tangential), ft/sec	1474
Bypass ratio	3.8
P/P overall	1.82
Fan adiabatic efficiency, overall	≥0.895
Stall margin	15 percent
Hub/Tip ratio	0.35
Rotor blade count	22
Stator vane count	52

Quiet High Speed Fan

The Quiet High Speed Fan (QHSF) had the goal of eliminating or reducing MPT noise while maintaining the same performance as the baseline fan. Therefore, the fan design parameters were the same as those provided for the baseline fan shown in figure 1. The sweep of the fan is intended to reduce the inflow Mach number normal to the leading edge to a value of approximately 0.92, therefore eliminating the leading edge shock and reducing MPT noise. In addition, the design is intended to contain the passage shock to the maximum extent possible, also with the intent of reducing MPT noise. A picture of the resulting forward swept fan in 22 in. model size is shown in figure 2.

Test Configurations

The test configurations developed using hardware for these fans were designed for the NASA Glenn Research Center 9- by 15-Foot Low Speed Wind Tunnel (ref. 5) and the NASA Ultra High Bypass (UHB) drive rig (ref. 6). Testing of acoustic concepts has included the use of several configurations of the same basic model to acquire various types of research data making efficient use of the model hardware and program funds. For this wind tunnel test entry, two primary model configurations were used that include a performance configuration and an acoustic configuration for acquiring aerodynamic performance and far-field acoustic data, respectively. Various other derivative configurations were used to acquire Laser Doppler Velocimetry (LDV) data (ref. 7), over-rotor dynamic pressure data, and duct acoustic mode measurements (ref. 8). Both primary model configurations include the appropriate fan stage mounted on the UHB drive rig. The model incorporates a passive core to simulate the flow that would enter the engine gas generator section. This air is also reintroduced into the bypass flow stream prior to exiting the engine typically referred to as a mixed flow exit nozzle. The bypass ratio for the engine cycle simulated by this model varies significantly. The model uses a translating spool piece that varies the bypass duct exit nozzle area to throttle the core and allow a range of bypass ratios to be set by the model operator. The non-structural guide vane section for these models is located upstream of the flow path splitter and therefore extends across the full span dimension of the flow path. To support the model nacelle, a fan frame is used consisting of 10 struts that extend though both the bypass and core flow duct. The flow path splitter is included as an integral part of the fan frame strut. The strut design is a direct scaled version of the part used in the TFE731-60 engine. The composite guide vane fabrication and mounting is similar to that used in the engine system.

Performance Configuration

The performance model configuration uses a bellmouth inlet and a variable fan exit nozzle (VFEN) as shown in figure 3. Typically the model skins are not installed for this configuration to allow instrumentation access and installation of probes, etc. The bellmouth is required to condition and accurately measure the mass flow entering and passing through the internal flow path of the model. The variable fan exit nozzle (VFEN) is used to set the model exit area, or back pressure, to allow testing at all fan stage operating conditions ranging from choke at the high flow end of a speed line to stall (or other limiting condition) at the low flow end of a speed line. In addition to these components, some of the instrumentation locations are also identified on figure 3 for the total pressure measurements (PT), the total temperature measurements (TT), and the static pressure measurements (PS). As noted in the figure, the stage performance instrumentation includes frame mounted probes that include a total pressure and total temperature sensor within a common probe bugle. These frame mounted probes include 10 radial probe locations with 6 of these located in the bypass duct and 4 located in the core duct. A photo of one of these vane mounted probe arrays is shown in figure 4. These are all mounted on the fan frame located just downstream of the guide vanes. Inlet boundary layer rakes, shown in figure 5, were used to measure the boundary layer for both the bellmouth inlet and the flight inlet. One additional configuration tested included the VFEN and the flight inlet with all other model parameters as shown for the performance configuration to obtain inlet boundary layer data. This used the same model configuration to get boundary layer data for both the flight inlet and bellmouth inlet.

Acoustic Configuration

The acoustic configuration is the most “flight-like” configuration tested for this model. The inlet and nozzle are designed like those on a typical business jet application. Figure 6 shows a cross section of the acoustic configuration. All of the external skins remain in place during all phases of far-field acoustic testing. The acoustic configuration is shown in figure 6. The stage performance instrumentation, located on the fan frame, remained in place during acoustic testing and was used to monitor stage pressure rise

and to calculate bypass ratio. A weight flow curve fit was used for the fan frame instrumentation to measure weight flow through the bypass and core ducts.

Results

Baseline Fan Stage Operating Map

Each fan stage was installed and the stage operating map measured using the model performance configuration previously described. The baseline fan was tested first since it was deemed to have the least risk over the expected operating range. Figure 7 shows the measured baseline operating map. The sea level static (SLS) and altitude (ALT) operating lines are shown for reference. Strain gages are installed and used for monitoring the structural response of fan blades during model checkout and high strain test events such as stall. The baseline fan blades had limited instrumentation resulting in a constrained set of test conditions to assure some operational gages remained throughout test phases requiring structural monitoring. Therefore, to conserve strain gage instrumentation operating life, only 3 speed lines, 50, 75, and 100 percent fan corrected speed, were measured to the operability limit of the fan which for this case appeared to be rotating stall. Previous testing indicated this fan would stall at the approximate weight flow/pressure rise boundary as measured for the 22 in. test article. On the design operating line, the baseline fan weight flow was 97.97 lb/sec at a pressure ratio of 1.756. These values are 0.9 and 3.1 percent low, respectively; relative to the design goals shown in table 1 (assumes a stage pressure ratio of 1.78 at the design point). The measured stage adiabatic efficiency map is shown in figure 8. The fan map efficiency plots include the adiabatic efficiency measured for operating line points using the fixed nozzle for speeds at or below 90 percent corrected speed and for VFEN points on the altitude operating line for speeds above 90 percent corrected speed. Since the fans are not designed to run below 90 percent at sea level, these efficiencies seemed the most appropriate way to characterize the fan performance. The measured stage efficiency is significantly lower than expected for the 22 in. baseline fan stage. The peak efficiency at 100 percent speed was 83.3 percent at a weight flow of 97.96 lb/sec (essentially on the operating line). If one assumes a reasonable value for guide vane efficiency, these measurements indicate the stage efficiency is approximately 4.2 percent lower than expected (rotor design goal of 89.5 percent minus 2 percent for guide vane gives 87.5 percent for the stage). Follow-on testing utilizing rotor survey probes allowed limited data to be acquired to investigate the source of the efficiency deficit. The additional data for the rotor was to be acquired in the hopes of determining whether the rotor or stator was the most likely cause of the lower efficiency. This is discussed in a later section of this paper.

QHSF Fan Stage Operating Map

The QHSF measured operating map is shown in figure 9. For this fan, an attempt was made at each speed to reach the anticipated stall line, however, at all test speeds above 50 percent and below 95 percent fan corrected speed, an instability was encountered that severely limited the operating range of the fan. At 50, 95, 97.5, and 100 percent fan corrected speed, the fan limiting condition appeared to be stall. This was inferred by the strain gage data showing broadband excitation at, or near, the expected stall line. At all other speeds tested, an instability causing high strains limited the operating range of the fan. The instability had, for some cases, characteristics similar to classical flutter. Considerable post test analysis was completed for this fan and is included in references 9 to 13. Since these papers cover this topic exhaustively, no further discussion is included in this paper. For 100 percent fan corrected speed on the design operating line, the QHSF weight flow was 98.28 lb/sec at a pressure ratio of 1.764. These values are 0.7 and 2.1 percent low, respectively; relative to the design goals shown in table 1 (assumes a stage pressure ratio of 1.78 at the design point). The stage adiabatic efficiency map is shown in figure 10. The operating line efficiency on the plot was generated in the same manner as used for the baseline fan. The peak stage efficiency at 100 percent speed was 85.9 percent at a weight flow of 98.18 lb/sec (again, essentially on the operating line). Just as for the baseline fan, no rotor performance data were concurrently

measured during this test phase. However, the stage value for the QHSF is considerably better than the baseline fan, bettering its peak efficiency by 2.6 percent. Again, limited rotor survey data were acquired to determine the performance of the fan and whether it meant the design intent with respect to the fan design pressure ratio and efficiency goals. This is described in a later section of this paper.

Operating Map Comparison

The fan map for both the baseline and Quiet High Speed Fan are presented in figure 11 with data for both fans overlaid on the same scales. This allows a direct comparison of features of the fan performance along the speed lines acquired during performance testing. For each speed line, the QHSF fan performance is marked by increased weight flow and pressure rise when compared to the baseline fan for all operating speeds up to the 100 percent fan corrected speed data. At the design speed, the 2 fans exhibit similar performance along the choke portion of the speed line and deviate once the operating line is crossed with the QHSF continuing to a higher pressure ratio before rolling over toward the stall line.

Another obvious feature is the severe operating limits imposed by the flutter region for the forward swept fan. It was not until 95 percent fan corrected speed when the flutter boundary retreated allowing testing to continue along the speed lines to approach the stall line with the QHSF stage. Once at 100 percent speed, some range extension is indicated for the forward swept fan with measurements indicating approximately 3 percent stall margin improvement at design speed. One must note that stall testing along a speed line is terminated when stresses on the instrumented airfoils exceed pre-determined limits and therefore, there are associated variations in determining the exact point of stall.

Measured Acoustic Operating Line

In preparation for acoustic testing (ref. 14), the wind tunnel models are tested with the flight nozzle and the bellmouth inlet installed inlet to get an accurate weight flow measurement along the acoustic operating line. For this model, the nozzle design facilitated trimming to get to the proper operating conditions. After trimming, both fans were operated with the final trimmed nozzle and the operating line characteristics determined. Figure 12 shows weight flow versus stage pressure rise plotted for both the baseline and QHSF along this fixed nozzle operating line. The 2 fans track nearly identical operating lines until the higher speeds are approached where the baseline fan has a higher pressure rise for a given weight flow. A similar plot is shown in figure 13 which is the pressure rise versus corrected tip speed. This plot shows the QHSF has a higher pressure rise for a given tip speed up to approximately 90 percent fan corrected speed where the 2 fans are approximately equal in pressure rise. After 90 percent speed the baseline fan produces higher pressure rise for a given tip speed.

Rake Performance Data

Inlet Boundary Layer

For completeness, the inlet boundary layer data are presented. These data were not used to correct any of the subsequent fan inlet pressure conditions but are included to document the differences between the outer duct boundary layer present on the flight inlet and the bellmouth inlet configurations. All of the data were acquired with a tunnel free stream velocity of Mach 0.05. Measurements of boundary layer data are presented in figures 14 through 16. Valid total pressure values from each of the 5 rakes were averaged to get a single boundary layer profile. The average boundary layer for the bellmouth inlet is shown in figure 14 at operating points of 75, 85, and 100 percent corrected speed. The radial coordinate of the flow path wall at the rake measurement plane is also plotted since the rake element positions are specified in radial distance from the model rotational centerline. The boundary layer depth grows as the operating speed increases from 75 to 100 percent corrected speed but the depth remains nearly constant at approximately 0.467 in. for the bellmouth inlet. Figure 15 shows the boundary layer thickness at nearly

the same operating conditions but with the flight, or acoustic, inlet installed. For this configuration, the boundary layer depth again increases with speed; however the thickness of the boundary layer is noticeably thicker at the 100 percent corrected speed operating condition as compared to the 77 and 84 percent corrected speed conditions. For the lower rotational speeds the boundary layer thickness is approximately 0.467 in. which matches the thickness using the bellmouth inlet. For the 100 percent corrected speed condition, the boundary layer is considerably thicker measuring between 0.921 and 1.067 in. in thickness. The exact value is between the fixed measurement probe locations. The reason for the significant increase is unknown but is likely due to poor flow characteristics near the inlet lip at the free stream Mach number used for this test configuration. Since the engine does not take off at 100 percent engine speed, this condition is not typical of ground operations at low forward velocities.

Stage Measurements

The stage performance for the baseline and QHSF fan test articles was measured using rake data acquired using fan-frame mounted total pressure and total temperature probes mounted in a common bugle as previously shown in figure 4. Since this instrumentation remains installed in the acoustic configuration, the rake data presented are using the fixed nozzle and bellmouth inlet and represent operation on the acoustic operating line. The bellmouth allows the most accurate weight flow measurement in the fixed nozzle configuration. All rake data are presented, through 100 percent corrected speed, using the fixed nozzle and bellmouth configuration used to define the flight nozzle area trims. In the fan map data section of this paper, a mix of fixed nozzle and VFEN data was used to characterize efficiency over the operating line on the efficiency maps (figs. 8 and 10) since the engine only runs at 100 percent corrected speed at altitude. The rake data presented in the following sections are plotted for the fixed nozzle configuration, through 100 percent corrected speed, since this is how all of the acoustic data were acquired. Another effect worth noting is that the fan exit guide vane wakes cause significant variation in probe measurements as they intersect the fan-frame mounted probes. Additionally, as the fan is operated at different speeds, the spatial location of the intersection of the wake with the probes varies slightly. These wake effects are the source of significant variation in the measured values at a specific circumferential location. Figure 17, showing individual stage total pressure rake profiles, displays this variation at 100 percent fan corrected speed for both fans. As is evident by the figure, the value at a single radial station can vary significantly depending on the circumferential location of the probe making the measurement. This difference is assumed to be caused by the probes location relative to the wake exiting the upstream guide vane. From the figure, a variation of approximately 0.1 in pressure ratio is typical, i.e., at the 9.727 in. radial location the pressure rise measured ranges from 1.703 to 1.811 for the baseline fan and 1.551 to 1.733 for the QHSF. Also, a repeat data point is plotted and shows that the values repeat very well for a repeat data point at the same operating condition. The data in figure 18, showing individual total temperature rake profiles, present the temperature data on a similar plot. The measurement of stage total temperatures includes a correction for probe recovery but no wire correction has been applied. The temperature variation from rake to rake is smaller but is easily observed in the data. At the same 9.727 in. location, the temperature ratio ranges from 1.201 to 1.244 for the baseline fan and 1.183 to 1.225 for the QHSF. These variations are present at all speeds and therefore may influence the radial average data presented in the following sections.

The total pressure was measured at several speeds for the baseline and QHSF in the acoustic configuration. Figure 19 shows a comparison of the area averaged radial total pressure profile for 65 to 100 percent corrected speed. This plot includes both the core and bypass instrumentation with the first 4 probes being located in the core passage and the outer 6 probes located in the bypass duct. At design point for 100 percent speed, the loading profile shows the baseline fan carries much more pressure rise near the tip as compared to the forward swept QHSF. The loading profiles cross at, approximately, the 9.165 in. probe radial location. Inboard of this location the baseline fan has lower loading than the QHSF and outboard the trend is reversed. Figures 20 to 24 show the individual area-averaged pressure ratio profiles at 65, 78, 81, 90, and 100 percent corrected speed.

Concurrently with the pressure measurements, the total temperature was measured at several speeds for the baseline and QHSF in the acoustic configuration. Figure 25 shows a comparison of the area averaged radial total temperature profile for rotational speeds of 65 to 100 percent corrected speed. As for the total pressure profiles, this plot includes both the core and bypass measurements. Again the first 4 probes are located in the core passage and the outer 6 probes are located in the bypass duct. These data are consistent with the pressure profiles. The plots show that for the baseline fan, more work is being done at the outer radii locations than for the QHSF. The temperature profiles cross slightly outboard of the 9.165 in. probe radial location where the pressure profiles crossed. Figures 26 to 30 show the individual area-averaged temperature ratio profiles at 65, 78, 81, 90, and 100 percent corrected speed.

Using the stage pressure and temperature ratio measurements, the fan stage adiabatic efficiency was calculated. Figure 31 shows baseline and QHSF stage adiabatic efficiency profiles for 65 to 100 percent corrected speed. The data show that the QHSF efficiency is higher at the outboard and inboard regions while the baseline fan had higher efficiency near mid-span of the bypass duct. Figure 32 to 36 show the individual adiabatic efficiency profiles using the area-averaged pressure and temperature values at 65, 78, 81, 90, and 100 percent corrected speed.

Rotor Survey Measurements

A follow-on test entry allowed limited rotor data to be acquired using two survey probes located just downstream of the fan trailing edge. Figure 37 shows the probe overall installation during model build-up. One probe was a wedge probe used to measure the swirl angle behind the rotor. This value was used to set the angle of the second probe, a combination total temperature and total pressure probe, which was used to acquire rotor pressure and temperature data. Figure 38 shows the combination probe mounted at the 18° location and the wedge probe located at the 90° location relative to top dead center. In figure 39, the wedge probe shown at the top left includes a total pressure tap flanked by 2 static pressure taps, one of which is visible in the figure. The notch just below the total pressure location includes a thermocouple (not used in data reduction) for total temperature measurement. Additionally, figure 39 shows the axial location of the measurement plane relative to the fan stacking line in the bottom of the figure.

Rotor Data

During a brief re-installation of the test hardware, limited rotor data were acquired in the performance configuration for each fan stage. The intent was to obtain rotor surveys for limited conditions for comparison to the baseline and QHSF stage data. Data were acquired at three operating speeds that include 59, 75, and 90 percent of the corrected design speed. These speeds correlate to the acoustic rating points, namely, approach, cutback, and takeoff. The rotor pressure profile is shown in figure 40 for the three data speeds and is plotted versus percent span. The low power speed, 58 percent fan corrected speed, indicates the loading between fans is similar but as the speed increases to 75 and 90 percent fan corrected speed, the loading for the forward swept QHSF is pushed notably inboard. This is consistent as the design intent was to reduce loading at the tip to enhance operability and stability while attempting to keep the outboard Mach numbers lower than the baseline fan to reduce MPT noise generation.

Data for the rotor temperature profile are shown in figure 41. Again the work being done on the fluid by the fan is greater inboard for the QHSF which is consistent with the pressure profile measurement. One's initial impression would question the mid-span temperature increase shown for the QHSF at 90 percent speed. The stage radial temperature profile for 90 percent corrected speed, shown in figure 29, has the same characteristic, although less pronounced, near the mid span region. Additionally, in looking at the data for an 18 in. version of the same fan (ref. 1), the local increase is observed there as well, indicating the effect is real and repeatable at 2 different scales with 2 different data systems.

The resulting efficiency profile using the rotor survey pressure and temperature data is shown in figure 42. These data indicate the efficiency near the root of the airfoil is similar for both the baseline –60 and QHSF fan designs. The part span efficiency of the forward swept fan is well below the baseline while at the tip the forward swept fan is improved relative to the baseline. The dip in efficiency that corresponds to the mid-span temperature rise is visible and consistent with the observations for the temperature survey data. The other notable information, from the rotor efficiency profiles, is that no significant efficiency deficit for the baseline fan is revealed that would account for the stage efficiency deficit through 90 percent corrected speed. Recall the stage data indicated a significant drop in efficiency for the baseline stage performance with an integrated efficiency of about 3 points lower as compared to the QHSF stage.

All of the integrated efficiency data acquired during the rotor survey tests is summarized in tables 2 and 3. Table 2 shows the efficiency deltas for the baseline and QHSF rotor and stage data acquired concurrently during the rotor surveys. Table 3 shows efficiency deltas for the baseline fan and stage data and QHSF fan and stage data, respectively. The 90 percent corrected speed rotor survey data indicate the QHSF rotor is operating at about 1.2 percent higher efficiency when compared to the baseline rotor. The stage data indicate the QHSF stage efficiency improved significantly over the baseline fan at 90 percent speed and is approximately 5.7 percent higher. A rotor survey was taken for only the baseline fan at 100 percent corrected speed and these data indicate the baseline fan efficiency drops markedly at the 100 percent speed condition missing the design intent by approximately 5.4 percent.

TABLE 2.—EFFICIENCY COMPARISON BETWEEN ROTOR AND STAGE DATA FOR EACH FAN (CONCURRENTLY MEASURED)

	Rotor			Stage		
	Baseline	QHSF	delta	Baseline	QHSF	delta
59 percent fan corrected speed	85.2 percent	85.7 percent	0.5 percent	79.6 percent	83.5 percent	3.9 percent
75 percent fan corrected speed	85.8 percent	85.9 percent	0.0 percent	80.1 percent	84.1 percent	4.0 percent
90 percent fan corrected speed	86.7 percent	87.8 percent	1.2 percent	81.2 percent	86.9 percent	5.7 percent
100 percent fan corrected speed	84.1 percent	N/A		80.8 percent	N/A	

TABLE 3.—EFFICIENCY COMPARISON BETWEEN BASELINE AND QHSF ROTORS (CONCURRENTLY MEASURED)

	Baseline			QHSF		
	Rotor	Stage	delta	Rotor	Stage	delta
59 percent fan corrected speed	85.2 percent	79.6 percent	–5.6 percent	85.7 percent	83.5 percent	–2.2 percent
75 percent fan corrected speed	85.8 percent	80.1 percent	–5.7 percent	85.9 percent	84.1 percent	–1.8 percent
90 percent fan corrected speed	86.7 percent	81.2 percent	–5.5 percent	87.8 percent	86.9 percent	–1.0 percent
100 percent fan corrected speed	84.1 percent	80.8 percent	–3.3 percent	N/A	N/A	

The final parameter measured for the rotor is the exit flow swirl angle. These data are shown in figure 43 for both the baseline and QHSF fans at 3 operating speeds including 59, 75, and 90 percent corrected rpm. The baseline fan exit swirl angle is uneventful over the span with an inboard swirl angle of 42.2° at 59 percent speed to 45.4° at 90 percent speed at the 10 percent span location. The swirl for the baseline fan decreases, in a near linear fashion, to a low value of 30.6° at 59 percent speed and 33.12° at 90 percent speed. These minimum values occur at span locations of approximately 75 to 80 percent span. The swirl angle then increases rapidly to 38.5° at 59 percent speed and 44.9° at 90 percent speed at the 96 percent span location. The QHSF fan has similar swirl at the inboard location with a swirl angle of 41.6° at 59 percent speed and 44.8° at 90 percent speed, again at the 10 percent span location. The swirl along the span of the QHSF blade includes a region of where the swirl angle is significantly higher relative to the baseline fan and imprints a sine wave character to the shape of the curve. This region shifts inboard with model rotational speed occurring between 45 and 85 percent span at 59 percent model speed and shifts to between 35 and 70 percent span at 90 percent model speed. The minimum value for the swirl angle for the QHSF rotor is 30° at 59 percent speed and 31.9° at 90 percent speed. The swirl angle then rolls on quickly and reaches a maximum value of 32.3° at 59 percent speed and 41.9° at 90 percent speed at 96 percent span. Another observation in QHSF data is the fluctuations of swirl angle at a specific span location are not consistent with rotational speed. For the baseline fan, the swirl angle increases with rotational speed at nearly all span locations. This trend holds true for the QHSF to a span near 60 percent where the swirl angle curves cross over one another and the swirl angle is larger for the 59 and 75 percent speed data by up to about 1.6° of swirl. In general, the increased swirl angle at inboard regions of the QHSF fan is consistent with the design intent to shift the tip loading inboard relative to the baseline fan.

The final charts generated for the rake data are maps that combine the stage data operating points with the integrated operating conditions measured with the rotor surveys. These are shown in figures 44 and 45. Figure 44 is the data plotted for the baseline fan and, as expected, the rotor survey data points lie well above the stage data. The integrated survey point at 59 percent differs slightly from the stage data speed of 60 percent corrected speed and the rotor point is only slightly above the stage speed line. At 75 percent and 90 percent corrected speed the rotor data is well above the stage speed line data while at 100 percent corrected speed the delta between rotor and stage narrows as compared to 75 and 95 percent conditions. The design intent is also plotted and indicates that the integrated data would suggest the baseline fan did not achieve the design operating condition missing the design weight flow and pressure rise by 0.77 and 1.76 percent, respectively. Figure 45 is a similar figure but for the QHSF stage and rotor and again, the integrated survey data points lie above the stage data on the pressure rise versus weight flow map, as expected. These data again show the rotor and stage data points being close at 59 and 60 percent corrected speed while the 75 and 90 percent corrected speed rotor data is well above the corresponding stage data points. Unfortunately, no rotor data was acquired for the QHSF 100 percent design speed so no quantitative comparison can be made with regard to meeting the design intent. A qualitative assessment would suggest the QHSF rotor is likely to have met the design objectives since the stage data indicate the stage misses the design intent with respect to weight flow and pressure rise by 1.53 and 1.07 percent, respectively.

Force Balance Measurements

The NASA Glenn Research Center UHB drive rig includes 2 force balances. The dynamic, or rotating, balance measures thrust and torque transferred through the fan blades and disk. The static, or nacelle, balance measures six force components associated with the nacelle, fan exit guide vanes, and any associated support struts or pylons, if applicable. The nacelle related forces measured are thrust, torque, normal force, normal moment, side force and side moment. For purposes of this report, only the thrust and torque components are presented for the static balance. Each of the balances are vendor calibrated over a load range corresponding to the balance capability. For this test, the rotating balance used was only calibrated to 2000 lbs but subsequent calculations showed the structure would remain linear through the

operating range of the forces expected during this test. Subsequent calibration to a higher load value indicated this was a valid assumption. Balance temperature changes during a tunnel run also effect the force measurements. A balance force offset correction is applied to the primary balance forces, these being torque and thrust, as a function of model balance temperature. This correction is a linear curve fit generated using pre-run and post-run zero speed data points for the force of interest and the associated balance temperature.

Balance Data

The most useful balance force data is acquired during acoustic testing as this is the configuration that employs the cleanest installation in the wind tunnel facility, especially with respect to the nacelle forces. The acoustic configuration uses the nacelle skins to reflect a "flight-like" condition with respect to the external geometry, exit nozzle, and instrumentation egress and the tunnel is operated at a Mach number of 0.1. In contrast, the performance configuration includes no skins, a variable area exit nozzle, and usually has numerous instrumentation wires and tubes that are routed either internally or most likely through an external strut or pipe exiting through the tunnel floor. These items serve to introduce errors in any forces measured during performance testing and therefore, only balance data from the acoustic configuration is presented.

The rotor thrust and torque measured for the Baseline and QHSF fans is shown in figure 46. The top figure shows the fan thrust as a function of rotor speed. The curves for each fan track closely at low and mid rpm operating points but the baseline fan thrust is notably higher at 97.5 and 100 percent speed. The error band for the thrust measurement is approximately ±1 percent (of measurement) which in this figure is about 1 symbol width (20 at 2000 lbs measured), implying the difference is real. The baseline fan thrust at 100 percent speed is 2034 lbs while the QHSF fan is 1975 lbs which equates to a 2.9 percent thrust reduction at 100 percent speed. The measured rotor torque indicates the QHSF fan requires more power at low and mid range speeds while the fans require, essentially, the same power at 100 percent speed. Again the balance torque accuracy is approximately 1 percent of indicated reading. At 100 percent speed, the torque for the baseline fan is 1118 ft-lb and the torque for the QHSF fan is 1122 ft-lb, 0.3 percent higher.

The nacelle thrust and torque data are shown in figure 47 for the baseline and QHSF fan stages. The nacelle force balance measurement is not as clean as the rotor balance due to instrumentation routed internally through the model and exiting aft toward the UHB drive rig strut. The fan frame pressure and temperature tubing and wiring exits internally and through a seal at the aft of the model bridging the metric and non-metric portions of the model. This results in additional error and data scatter as compared to the rotating balance. The plot at the top of figure 47 shows the nacelle thrust as a function of model speed. The nacelle thrust measured for the QHSF fan stage is notably higher than that measured for the baseline fan stage. Even though significant scatter is evident in the data the trends of the thrust level are visible. The baseline nacelle thrust force is 623 lbs while the QHSF nacelle thrust is 693 lbs, an increase of 11.2 percent. This is consistent with stage efficiency conclusions drawn from the aerodynamic data. The stage rake efficiency measurements indicated the baseline configuration was operating at lower efficiency relative to the QHSF fan stage. The rotor survey data indicated the baseline rotor efficiency was comparable to the QHSF rotor, pointing to the guide vanes as the source of the efficiency drop. These nacelle force balance data would indicate the guide vane for the baseline fan has increased drag relative to the QHSF guide vanes, therefore a lower thrust, caused by a loss in the baseline vane that is also the source for reduced stage efficiency. The nacelle torque comparison is shown in the lower part of figure 47. The baseline nacelle torque values operate below the QHSF nacelle through the lower and mid-rpm speeds but converge at 90 percent speed to nearly the same values for 95 to 100 percent corrected speed. At 100 percent corrected speed, the baseline nacelle torque is 1060 ft-lbs and the QHSF nacelle torque is 1041 ft-lbs or 1.7 percent less. The nacelle torque for both the QHSF and baseline fans is below the rotor torque values. A likely cause of this difference is that some torque load is being carried by the hydraulic lines feeding the core actuator on the nacelle. Every effort was made to provide isolation

between metric and non-metric components but the hydraulic lines were relatively stiff compared to other lines and tubing.

The final force balance plot shown in figure 48 shows the total thrust, the fan balance added to the nacelle balance, for the baseline and QHSF acoustic configurations. This plot indicates the baseline fan stage is operating at a slightly lower thrust as compared to the QHSF fan stage for most of the operating line. The baseline fan stage operates at, generally, 40 to 50 lbs less thrust compared to the QHSF fan through approximately, 95 percent corrected fan speed. For 97.5 and 100 percent speed, the drop in QHSF high-rpm rotor thrust is approximately equaled by the offset in baseline nacelle thrust. As a result, the 2 fan stages operate at nearly the same overall thrust for these 2 operating conditions. Specifically, at 100 percent corrected speed the baseline and QHSF fan/nacelle total thrust is 2670 and 2678 lbs, respectively. This difference of approximately 0.3 percent is less than the balance accuracy.

Tip Clearance

The tip clearance was measured for both the baseline and QHSF fans. The fan case could be shimmed axially to adjust the tip gap given the convergent flow path over the rotor. By adding shims, the outer flow path wall moved forward axially and the tip gap was decreased. Conversely, by removing shims the case moved axially aft and the tip gap was opened. This was one of the first models to run in the NASA GRC 9 by 15 LSWT that had this capability. It was also the first time NASA Glenn developed systems for optical tip deflection and eddy-current/capacitance sensor tip clearance were used to make measurements in a 9 by 15 LSWT model. The optical method was a concept devised using probes originally planned for deflection measurements. This system did not prove reliable and no data from that system is shown in this report. The eddy-current/capacitance system was used to track tip clearance through sensor sets mounted at 2 pitch-wise locations, one set at 18° and one set at 90°, both angles measured relative to TDC with positive angular direction CCW viewed forward looking aft. Each set consisted of three sensors mounted using the tip chord location for both airfoils to assure the correct relationship between the sensor and the blade tip. The sensors were mounted to measure tip clearance near the leading edge, at mid-chord, and at the trailing edge. The installation is shown at the top of figure 49 as viewed from outside the model casing. The bottom of figure 49 shows the leading edge eddy-current sensor and the mid-chord capacitance sensor from a viewpoint inside the duct flow path. These sensors were used with initial calibration curves during testing but additional work was done after the test to refine the calibration and final calibration data was used to process the data shown in figures 50 and 51. Figure 50 shows the tip clearance as a function of physical rotational speed for the baseline fan. Data in the top plot are for the 18° location and the bottom plot is for the 90° location. The fan was designed to have a uniform tip gap along the chord however the data indicate the fan runs tighter at the trailing edge than at the leading edge by approximately 0.010 in. The minimum tip gap was at the 18° location and was approximately 0.022 in. Each curve shown is a continuous average of all 22 airfoils and the increasing scatter in the data is evident by the width of the curve as it progressed toward higher rotational speeds. At both the 18° and the 90° sensor locations the leading edge and mid-chord tip gap converges to nearly the same value of approximately 0.034 in. at 18° and 0.036 in. at 90°. The trailing edge tip clearance closes to 0.022 in. at 18° and 0.032 in. at 90°. As shown in figure 51, the QHSF fan tip clearance also displayed a trend of more open clearance near the leading edge and closing down tighter at the trailing edge. The gap difference between leading edge and trailing edge was approximately 0.022 in. at the 18° location. The trailing edge sensor was non-functional at the 90° location for the QHSF fan test configuration so a difference could not be calculated. The minimum clearance for the QHSF fan was 0.008 in. at the 18° location and, assuming the same sensor trends, 0.026 in. at the 90° location.

Conclusion

The aerodynamic performance of two 22 in. diameter fans has been measured using a set of stage rake instrumentation, rotor and nacelle force balances, rotor survey instrumentation, and various static pressures used for weight flow and duct Mach number calculations. The rotor data is sparse due to a limited test entry available to acquire this data. One of the fans tested was a scaled model of the Honeywell TFE731-60 product fan. This fan served as the baseline for comparing the performance of an aggressively forward swept fan designed to match the baseline operating conditions but have reduced Multiple Pure Tone noise characteristics. The performance comparison was affected by an apparent problem with the baseline hardware which produced higher losses than expected. Comparisons of the baseline fan and stage performance indicate the losses are associated with baseline fan exit guide vane performance. There were no obvious problems observed with the guide vanes and installation was executed similar to the forward swept test article. The performance of the forward swept fan met expectations with respect to pressure rise and efficiency goals but had severe operability limitations due to flutter occurring at part speed outboard of the operating line starting near 55 percent fan corrected speed, nearly touching the operating line at 70 percent fan corrected speed, and finally subsiding near 95 percent fan corrected speed. The acoustic performance showed considerable benefit over the high tip speed operating regions of the fan. The goal was to reduce MPT noise through control of the passage shock and inlet normal Mach number. Preliminary results indicate the noise has been reduced yet the exact nature of the reduction remains under study.

References

1. Weir, D., "Design and Test of Fan/Nacelle Models Quiet High Speed Fan," Final Report: NAS3–27752, NASA/CR—2003-212370, July 2003.
2. Repp, R., Gentile, D., Hanson, D., Chunduru, S., "Design and Test of Fan/Nacelle Models Quiet High Speed Fan Design," Final Report: NAS3–27752, NASA/CR—2003-212369, July 2003.
3. Groeneweg, J.F., Sofrin, T.G., Rice, E.J., Gliebe, P.R., "Aeroacoustics of Flight Vehicles: Theory and Practice, 3 Turbomachinery Noise," NASA RP–1258, August 1991.
4. Hayden, R.E., Bliss, D.B., Murray, B.S., Chandiramani, K.L., Smullin, J.I., Schwaar, P.G., "Analysis and design of a High Speed, Low Noise Aircraft Fan Incorporating Swept Leading Edge Rotor and Stator Blades," NASA CR–135092, December 1977.
5. Arrington, E.A., Gonsalez, J.C., "Calibration of the NASA Lewis research Center 9- by 15-Foot Low Speed Wind Tunnel (1994) Test," NASA CR 195438, March, 1997.
6. Balan, C., Hoff. G.E., "Propulsion Simulator for High Bypass Turbofan Performance Evaluation," SAE Paper 931410, April 1993.
7. Podboy, G.G., Krupar, M.J., "Measurements of Blade-to-Blade Variations in Shocks Upstream of Both a Forward-Swept and Aft-Swept Rotor," NASA/TM—2006-213445, 2006.
8. Heidelberg, L.A., "Comparison of Tone Mode Measurements for a Forward Swept and Baseline Rotor Fan," NASA/TM—2003-212378, June 2003.
9. Panovsky, J., Bakhle, M.A., Srivastava, R., "Flutter Characteristics of a Forward-Swept Fan," Proceedings of the 7th National Turbine High Cycle Fatigue Conference, April 2002.
10. Srivastava, R., Bakhle, M.A., Keith, T.G., Jr., Stefko, G.L., "Flutter Analysis of a Transonic Fan," ASME Paper 2002–GT–30319, June 2002; also NASA/TM—2002-211818.
11. Srivastava, R., Bakhle, M.A., Keith, T.G., Jr., "Numerical Simulation of Aerodynamic Damping for Flutter Analysis of Turbomachinery Blade Rows," Journal of Propulsion and Power, vol. 19, no. 2, Mar.-Apr. 2003.
12. Bakhle, M.A., Srivastava, R., Panovsky, J., Keith, T.G., Jr., Stefko, G.L., "Flutter Calculations of an Experimental Fan," Paper US-2, International Forum on Aeroelasticity and Structural Dynamics, Amsterdam, June 4–6 2003.

13. Srivastava, R., Bakhle, M.A., Keith, T.G., Jr., Stefko, G.L., “Influence of Shock on Flutter Characteristics of Turbomachinery Blade Rows,” Paper US-41, International Forum on Aeroelasticity and Structural Dynamics, Amsterdam, June 4–6 2003.
14. Dittmar, J.H., Elliott, D.M., Fite, E.B., “The Noise of a Forward Swept Fan,” NASA/TM–2003-212208, November 2003.

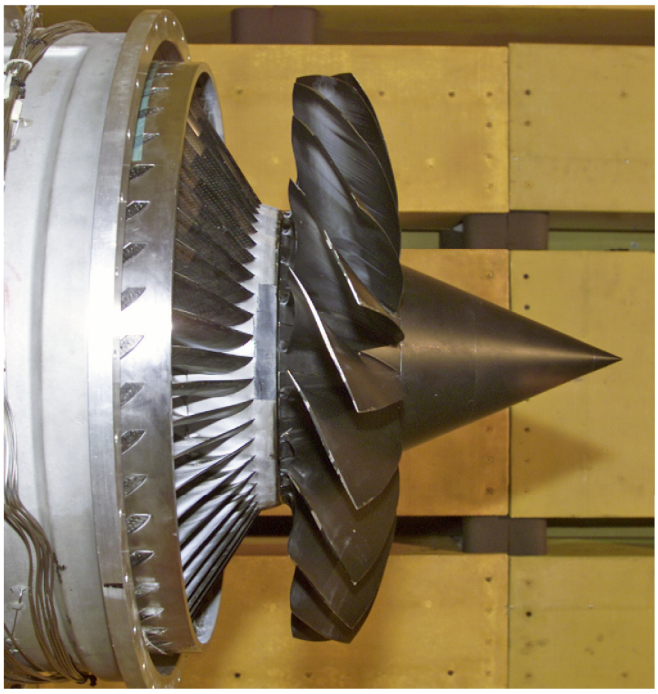

Figure 1.—Baseline fan, scaled TFE731-60 fan.

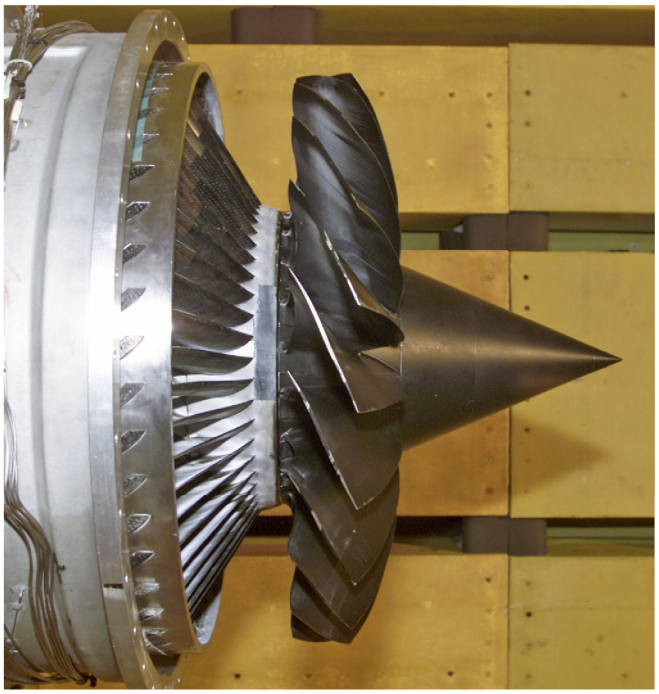

Figure 2.—Forward swept QHSF.

D059 AlliedSignal performance configuration, model aero instrumentation summary

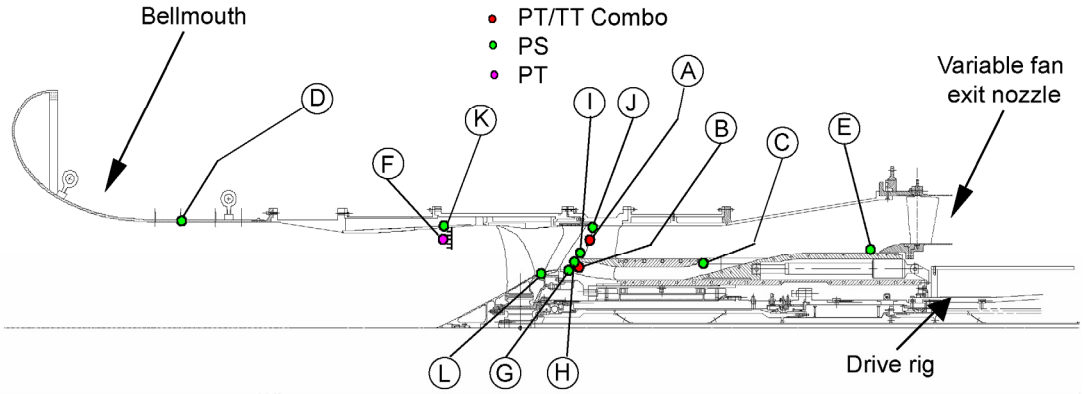

Location	Figure Locator	Instrumentation	Description
Fan Frame, Bypass	A	30 PT	stage bypass total pressure, 5 struts, 6 probes per rake
		30 TT	stage bypass total temperature, 5 struts, 6 probes per rake
Fan Frame, Core	B	20 PT	stage core total pressure, 5 struts, 4 probes per rake
		20 TT	stage bypass total temperature, 5 struts, 6 probes per rake
Core Nozzle	C	10 PS	core nozzle exit static pressure, core duct OD
Bellmouth	D	8 PS	bellmouth weight flow static pressures
Core Plug	E	10 PS	static pressure on the sliding plug OD flow surface, i.e., nozzle ID
Rakes, STA 2.0	F	50 PT	boundary layer total pressure
Core Inlet Fan Frame, ID	G	5 PS	static pressure for fan frame core ID
Core Inlet Fan Frame, OD	H	5 PS	static pressure for fan frame core OD
Bypass Inlet Fan Frame, ID	I	5 PS	static pressure for fan frame bypass ID
Bypass Inlet Fan Frame, OD	J	5 PS	static pressure for fan frame bypass OD
Inlet, STA 2.0	K	10 PS	static pressure at boundary layer rake location
Rotor Seal	L	4 PS	static pressure on forward facing plane aft of the rotor

Figure 3.—Performance configuration and associated instrumentation list.

Figure 4.—Fan frame mounted stage PT and TT bugles.

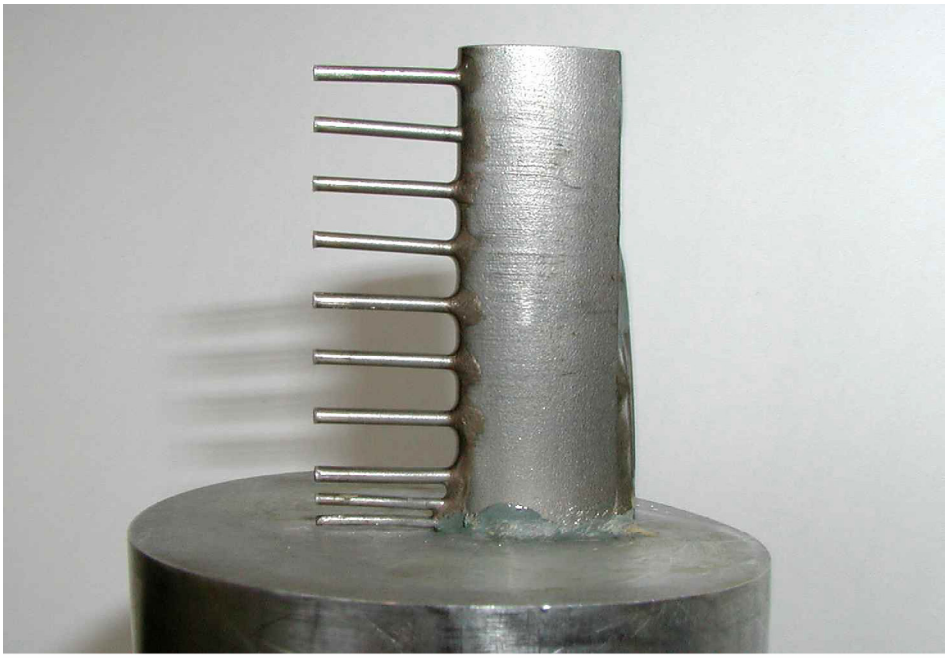

Figure 5.—Inlet boundary layer rake.

D059 AlliedSignal performance configuration, model aero instrumentation summary

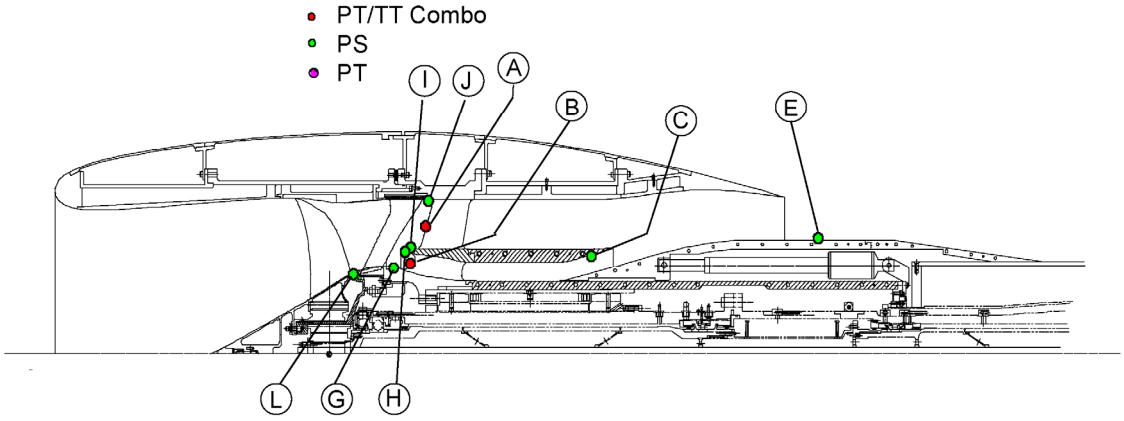

Location	Figure Locator	Instrumentation	Description
Fan Frame, Bypass	A	30 PT	stage bypass total pressure, 5 struts, 6 probes per rake
		30 TT	stage bypass total temperature, 5 struts, 6 probes per rake
Fan Frame, Core	B	20 PT	stage core total pressure, 5 struts, 4 probes per rake
		20 TT	stage bypass total temperature, 5 struts, 6 probes per rake
Core Nozzle	C	10 PS	core nozzle exit static pressure, core duct OD
Core Plug	E	10 PS	static pressure on the sliding plug OD flow surface, i.e., nozzle ID
Core Inlet Fan Frame, ID	G	5 PS	static pressure for fan frame core ID
Core Inlet Fan Frame, OD	H	5 PS	static pressure for fan frame core OD
Bypass Inlet Fan Frame, ID	I	5 PS	static pressure for fan frame bypass ID
Bypass Inlet Fan Frame, OD	J	5 PS	static pressure for fan frame bypass OD
Rotor Seal	L	4 PS	static pressure on forward facing plane aft of the rotor

Figure 6.—Acoustic instrumentation list.

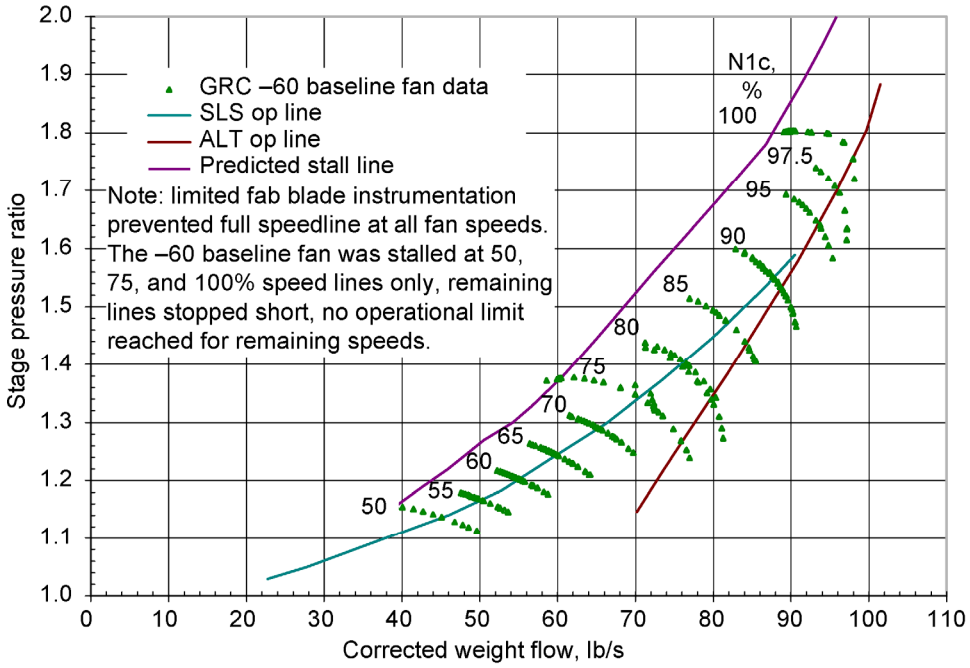

Figure 7.—Operating map for baseline fan, 22-in. tip diameter TFE731 –60 fan.

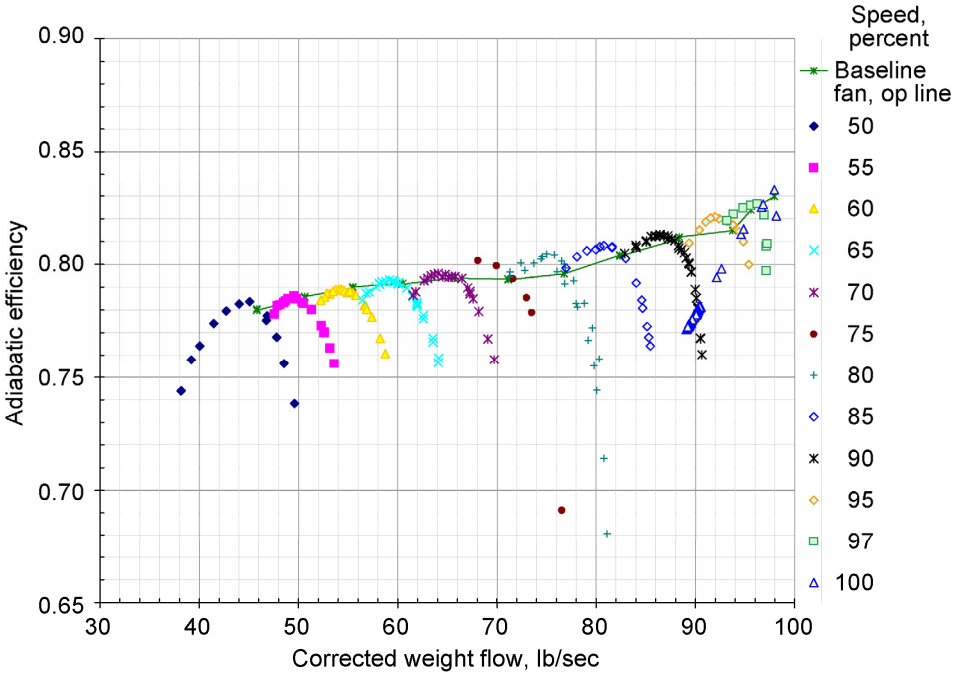

Figure 8.—Baseline fan stage adiabatic efficiency map (op lines shown for reference).

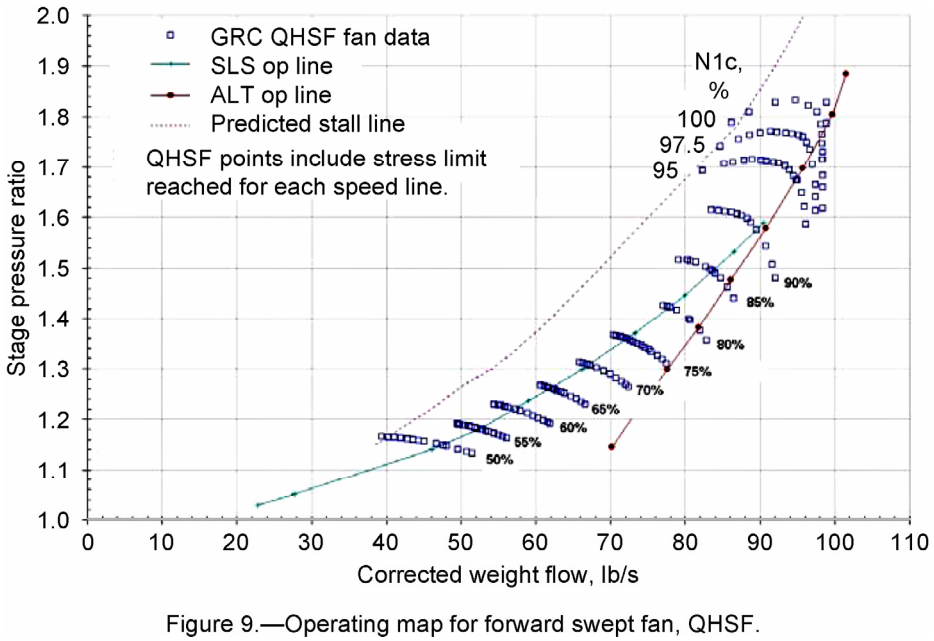

Figure 9.—Operating map for forward swept fan, QHSF.

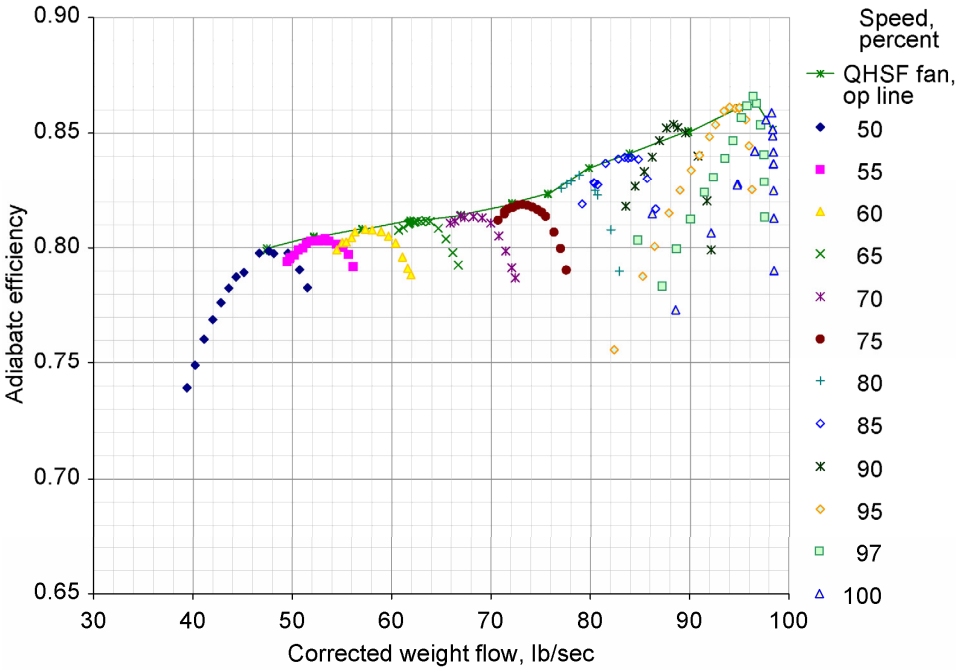

Figure 10.—Adiabatic efficiency map for forward swept fan, QHSF.

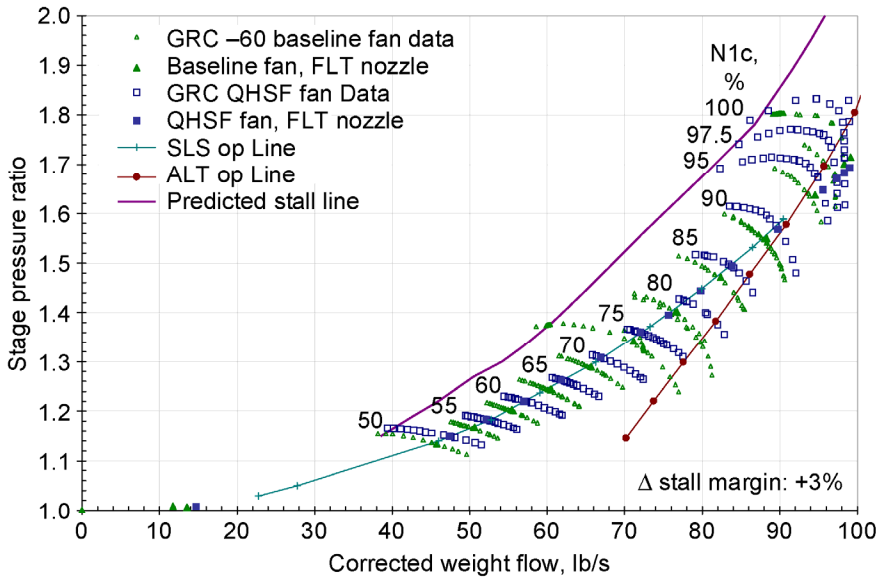

Figure 11.—Overlay of baseline and QHSF measured fan map. –60 Baseline fan stalled at 50, 75, and 100% speed lines only. QHSF points include stress limit reached for each speed line

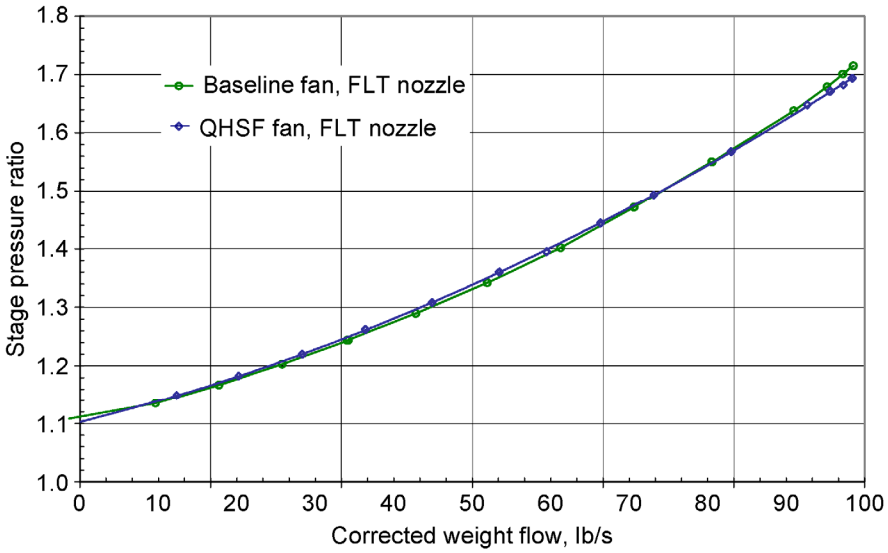

Figure 12.—Operating line comparison with the fixed nozzle.

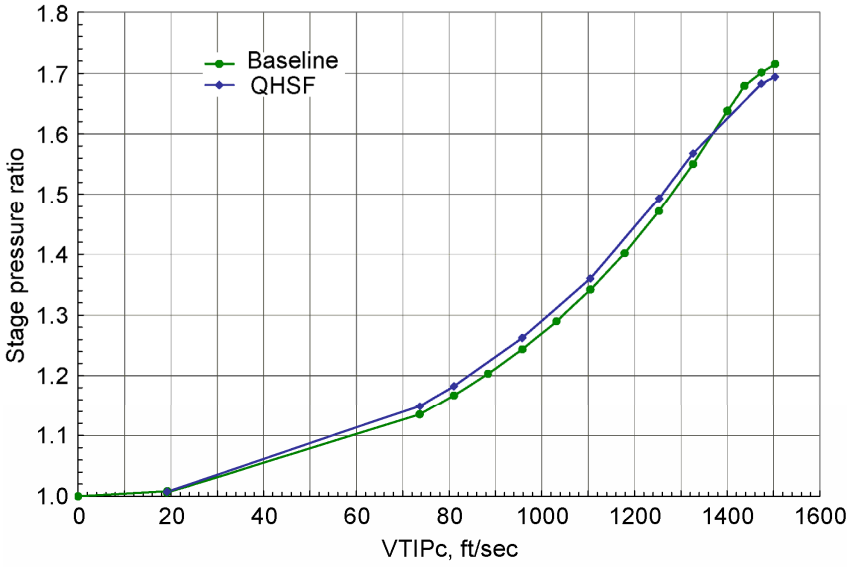

Figure 13.—Fan stage pressure rise as a function of tip speed.

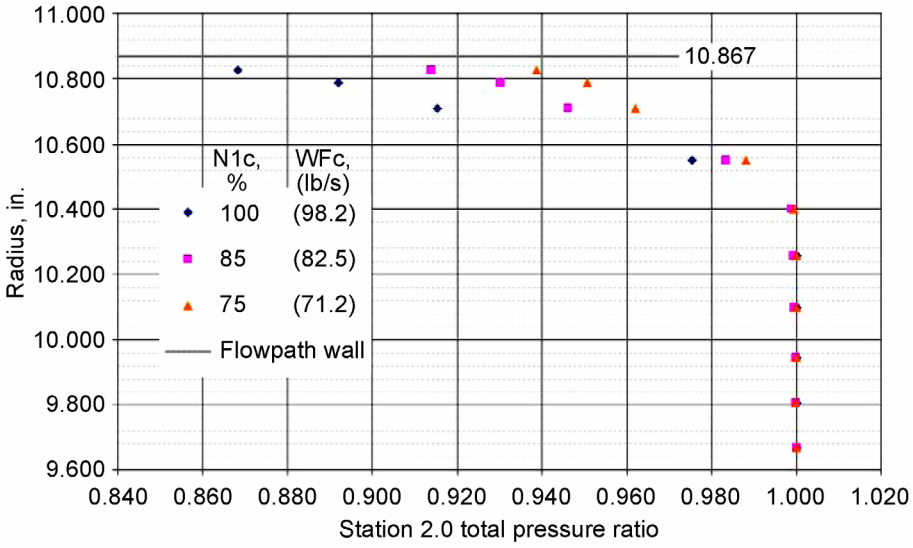

Figure 14.—Bellmouth inlet boundary layer, average of all rakes.

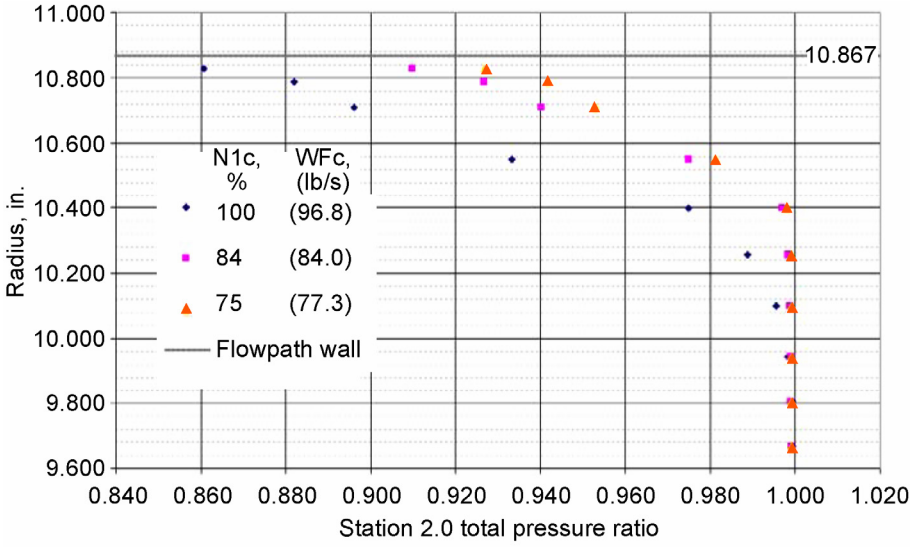

Figure 15.—Flight (acoustic) inlet boundary layer, average of all rakes.

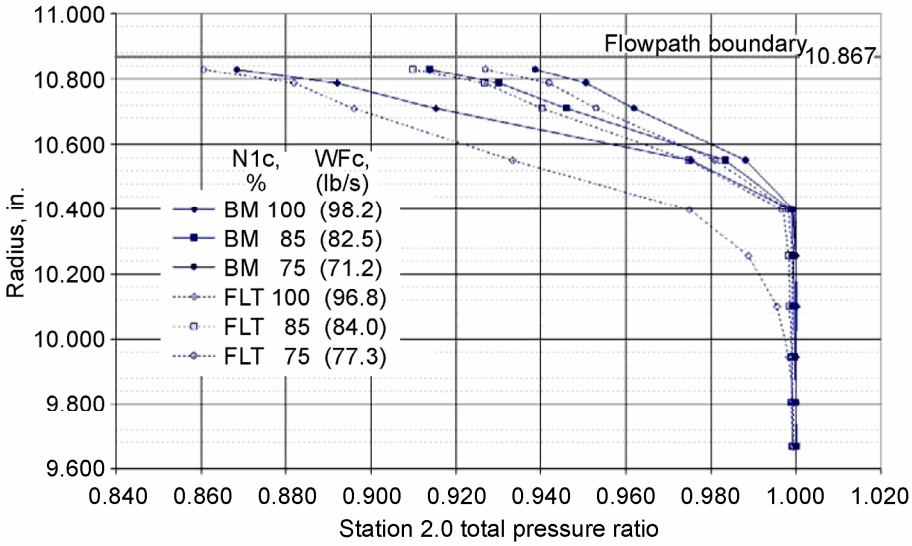

Figure 16.—Comparison of flight and bellmouth inlet boundary layer, average of all rakes.

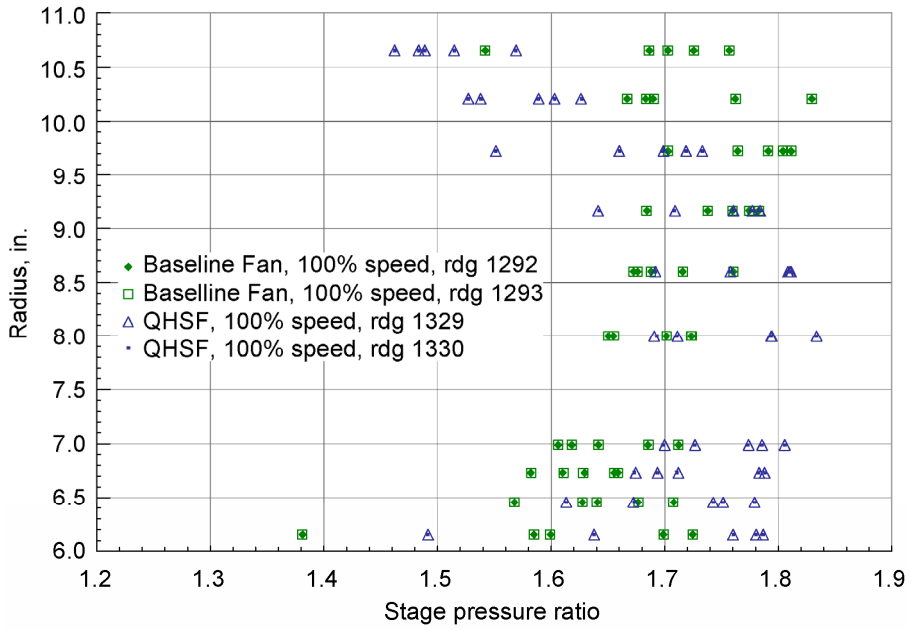

Figure 17.—Station 17 total pressure rake profiles, 100% speed.

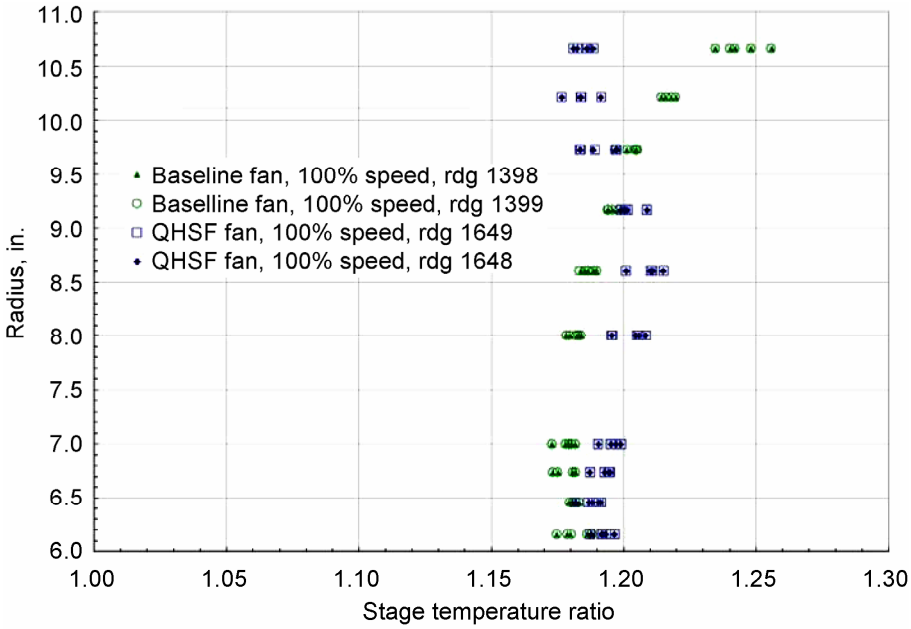

Figure 18.—Station 17 total temperature rake profiles, 100% speed.

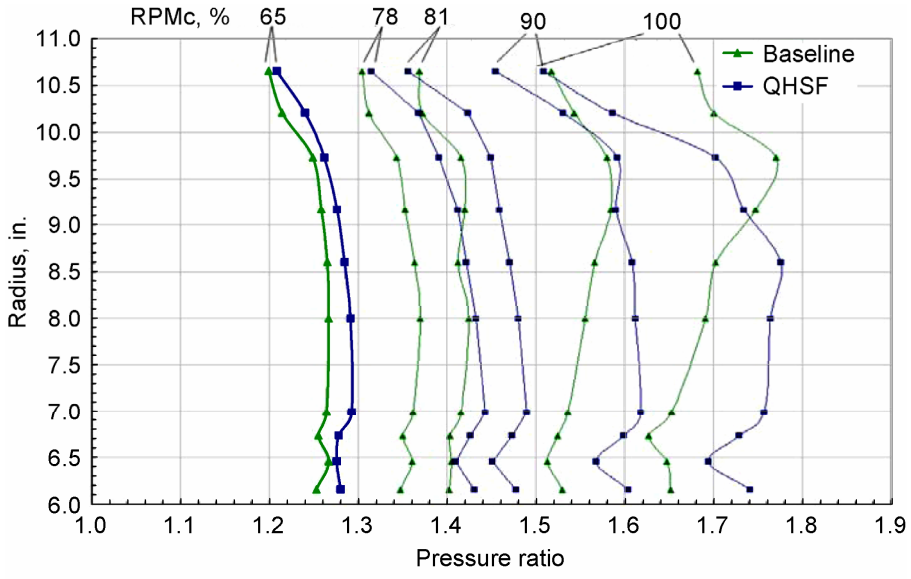

Figure 19.—Stage total pressure profiles over speed range.

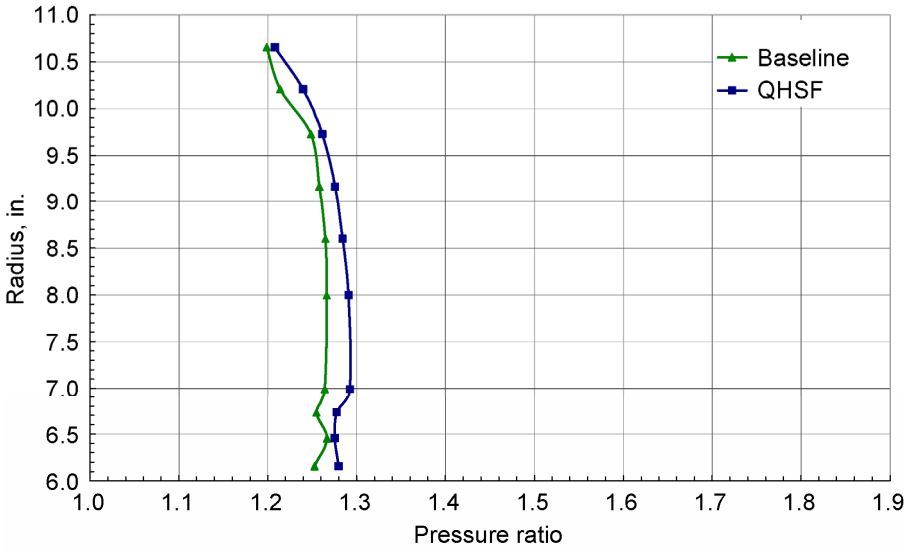

Figure 20.—Average total pressure profile, 65% RPMc.

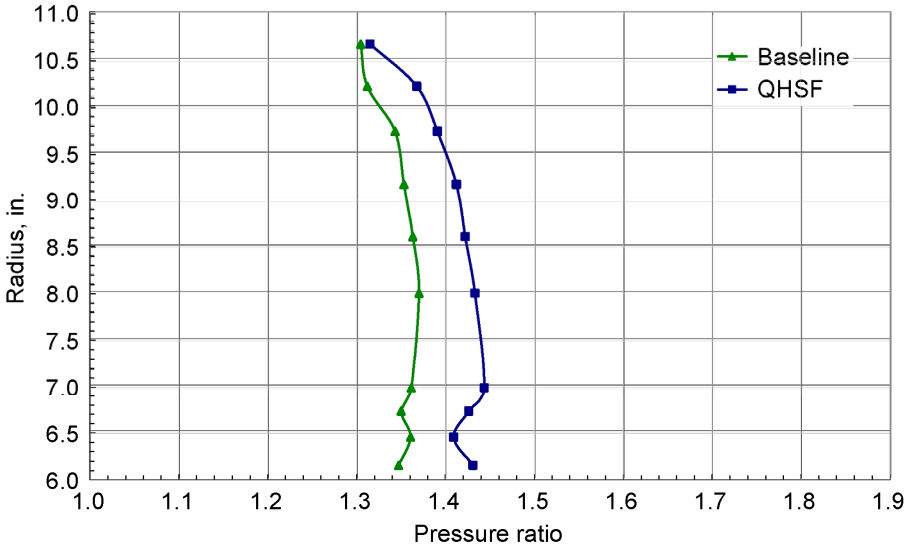

Figure 21.—Average total pressure profile, 78% RPMc.

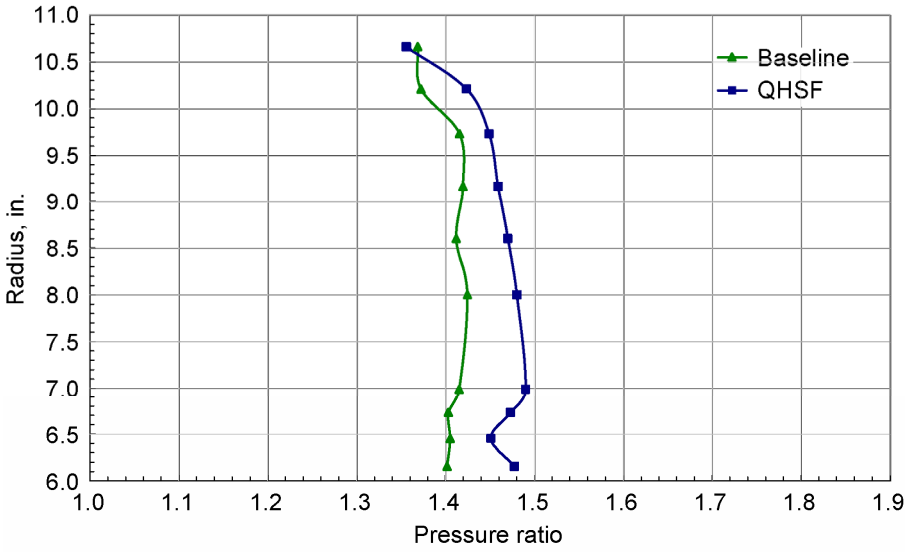

Figure 22.—Average total pressure profile, 81% RPMc.

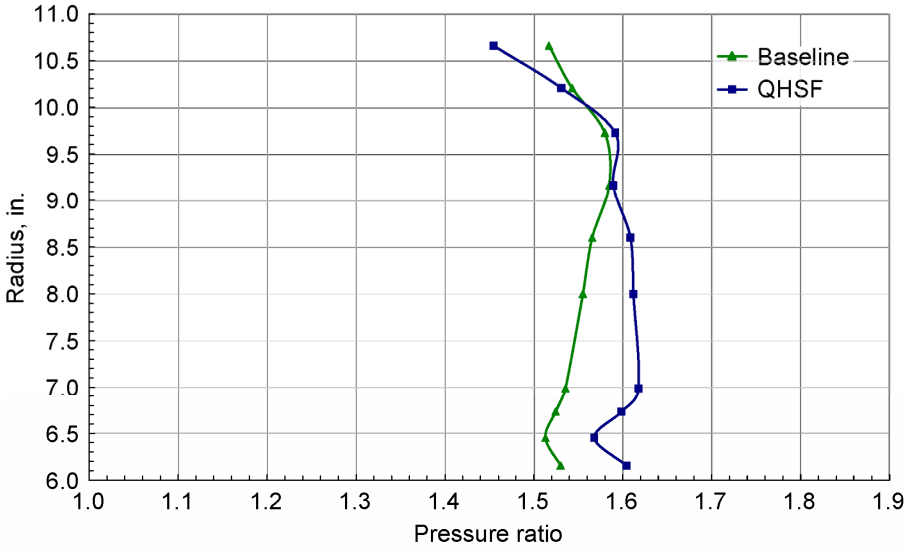

Figure 23.—Average total pressure profile, 90% RPMc.

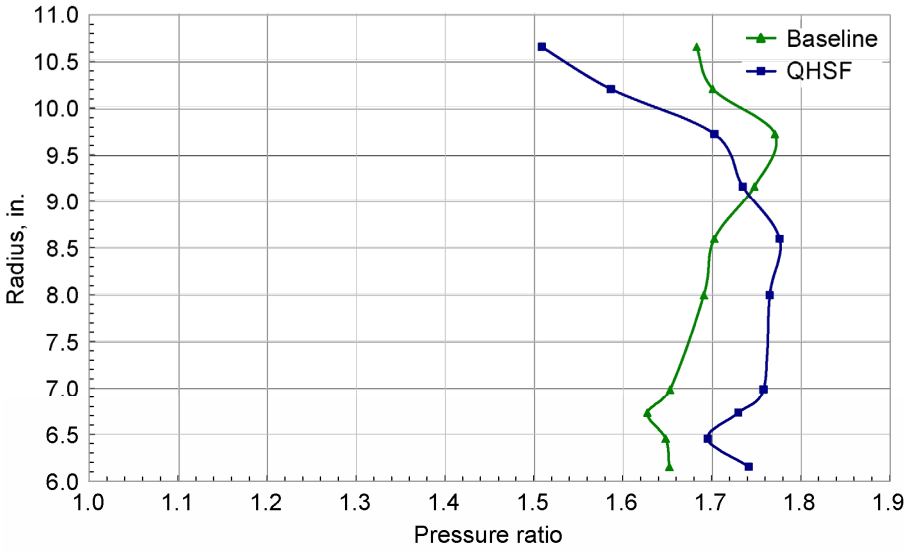

Figure 24.—Average total pressure profile, 100% RPMc.

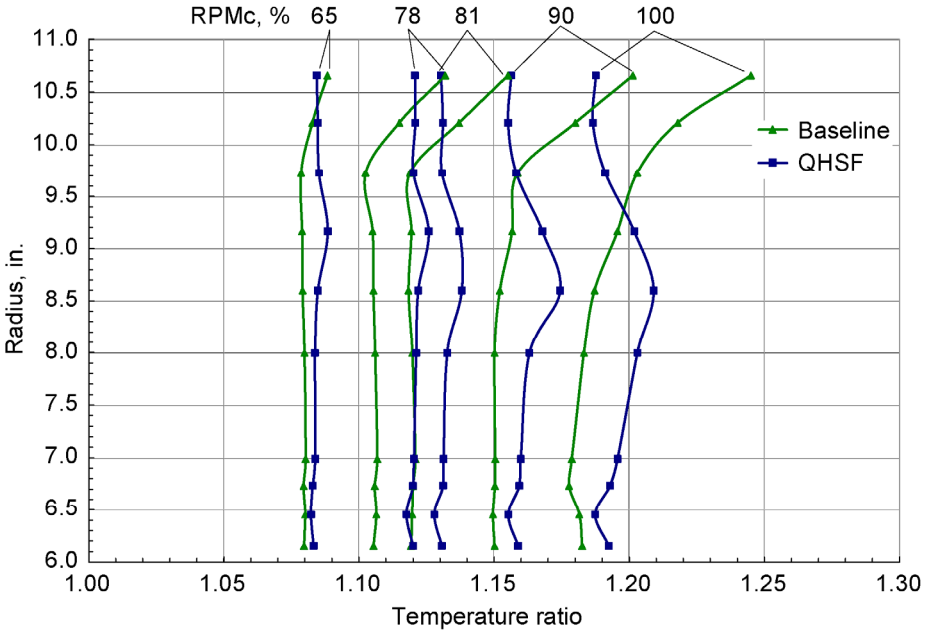

Figure 25.—Average total temperature profiles over speed range.

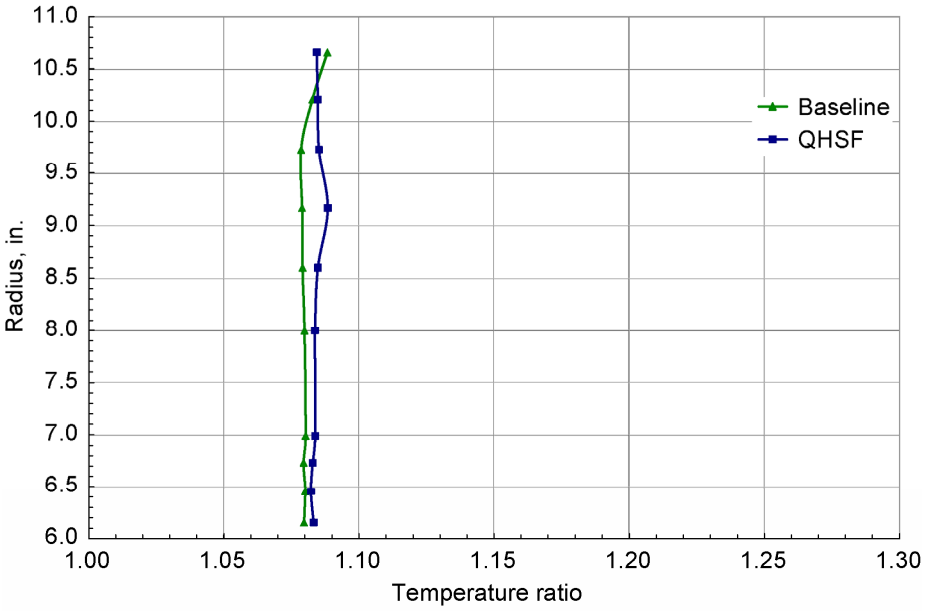

Figure 26.—Average total temperature profiles, 65% RPMc.

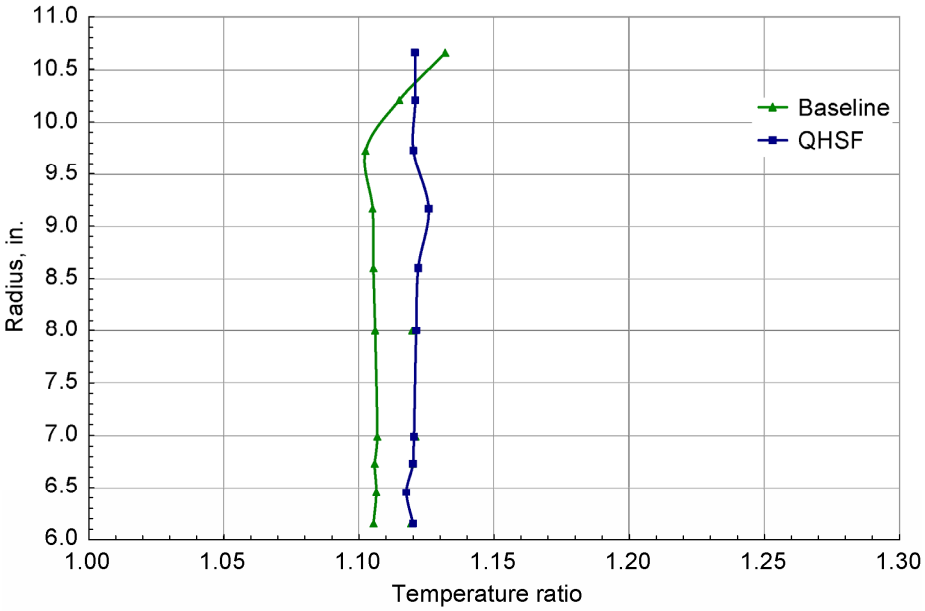

Figure 27.—Average total temperature profiles, 78% RPMc.

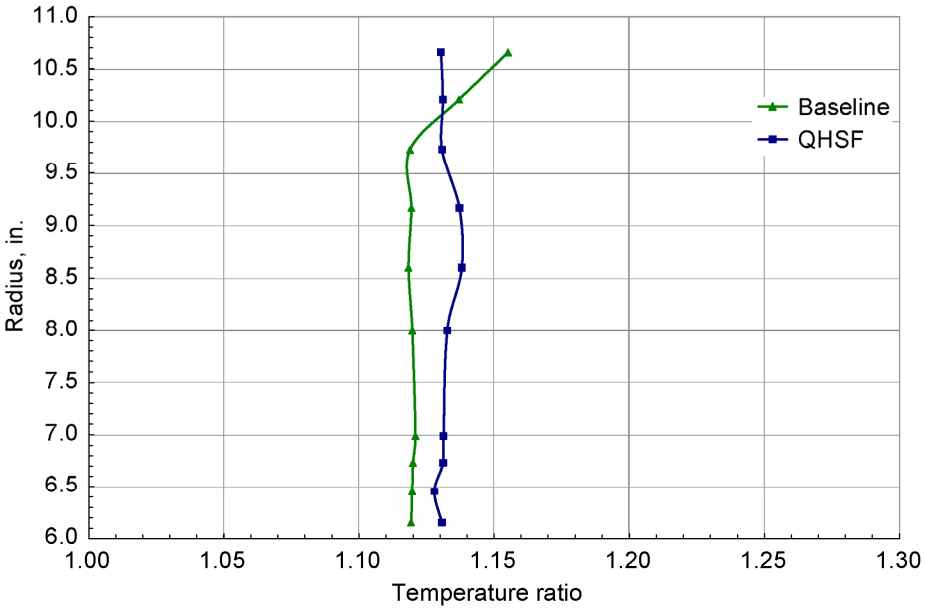

Figure 28.—Average total temperature profiles, 81% RPMc.

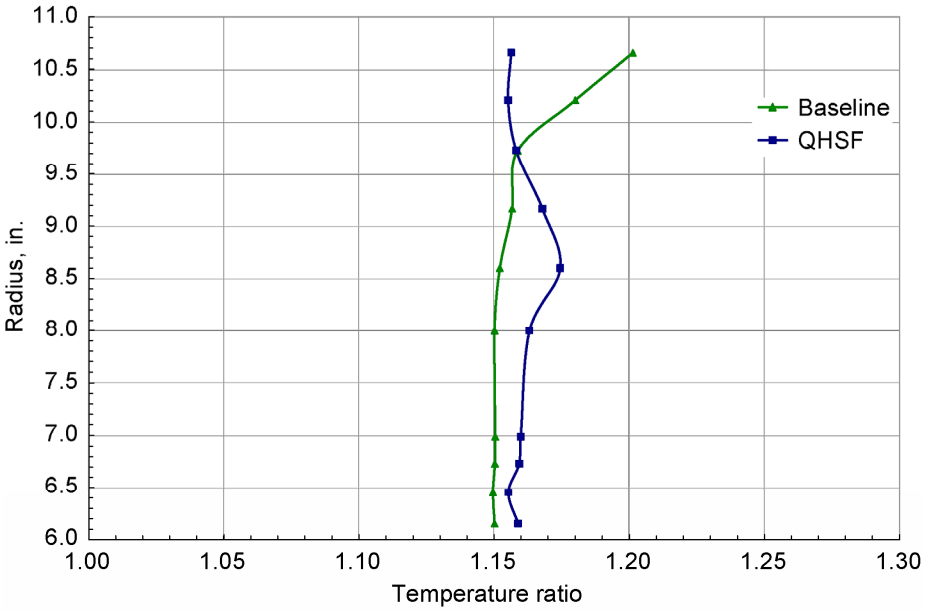

Figure 29.—Average total temperature profiles, 90% RPMc.

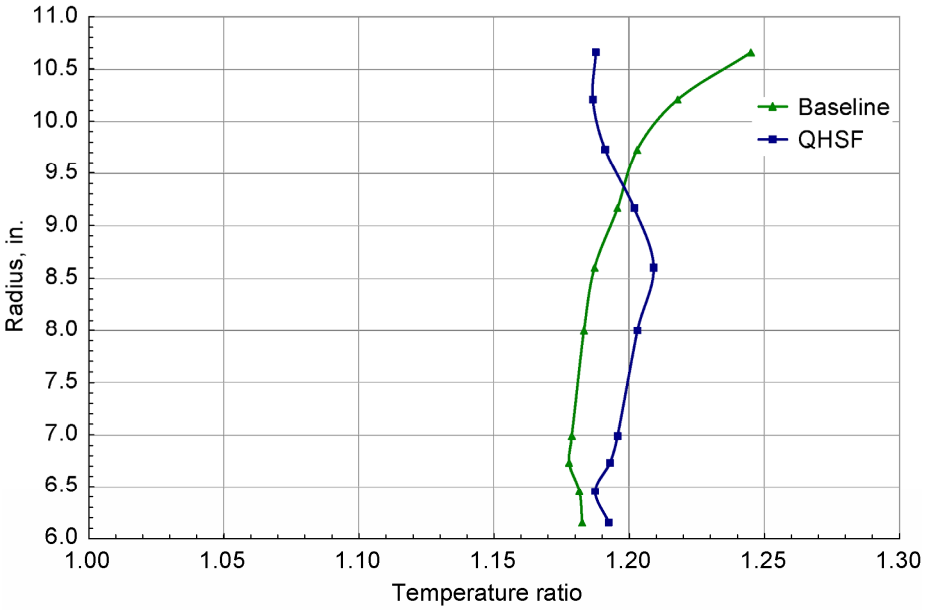

Figure 30.—Average total temperature profiles, 100% RPMc.

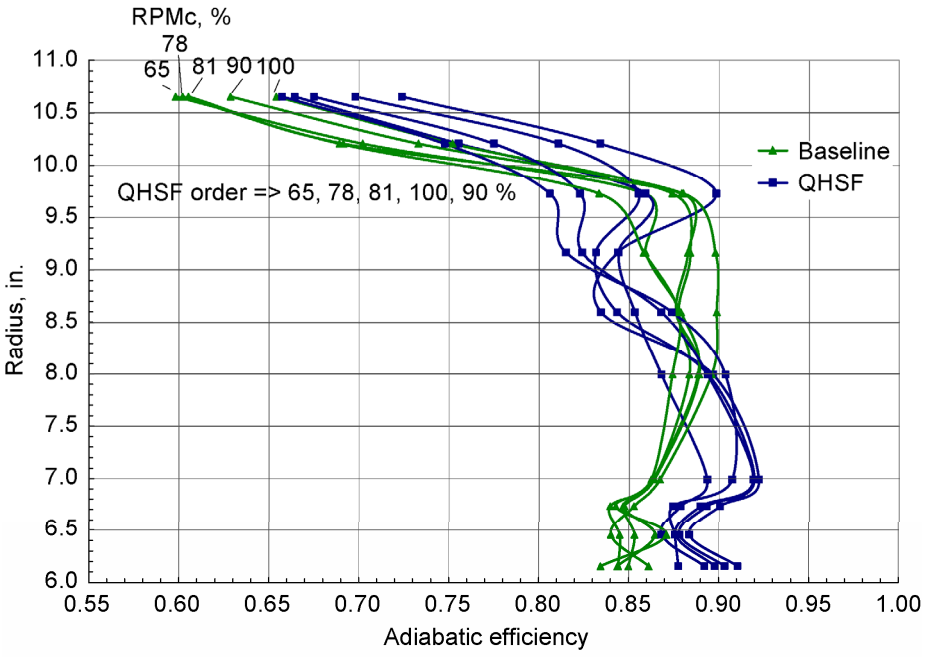

Figure 31.—Adiabatic efficiency profiles over speed range.

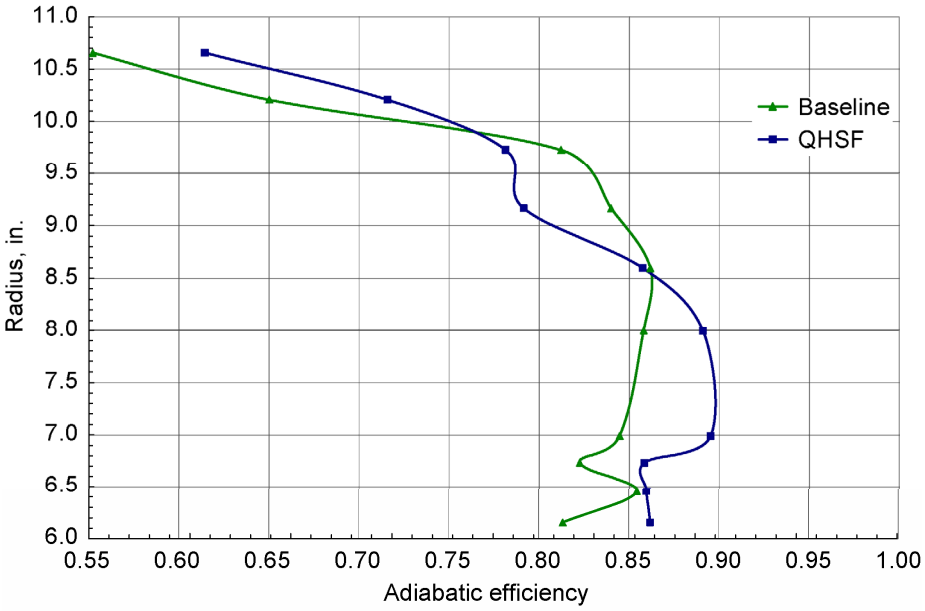

Figure 32.—Adiabatic efficiency profiles, 65% RPMc.

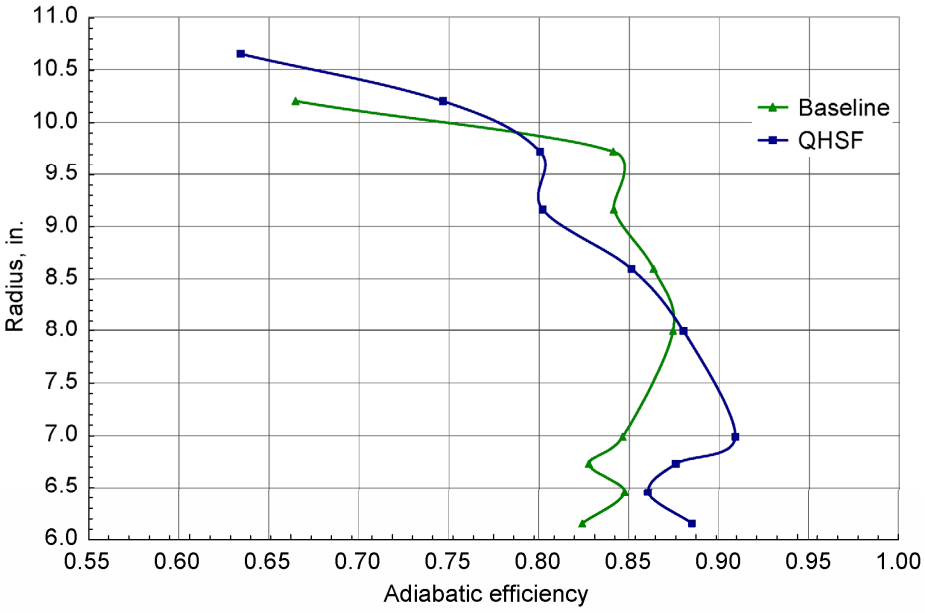

Figure 33.—Adiabatic efficiency profiles, 78% RPMc.

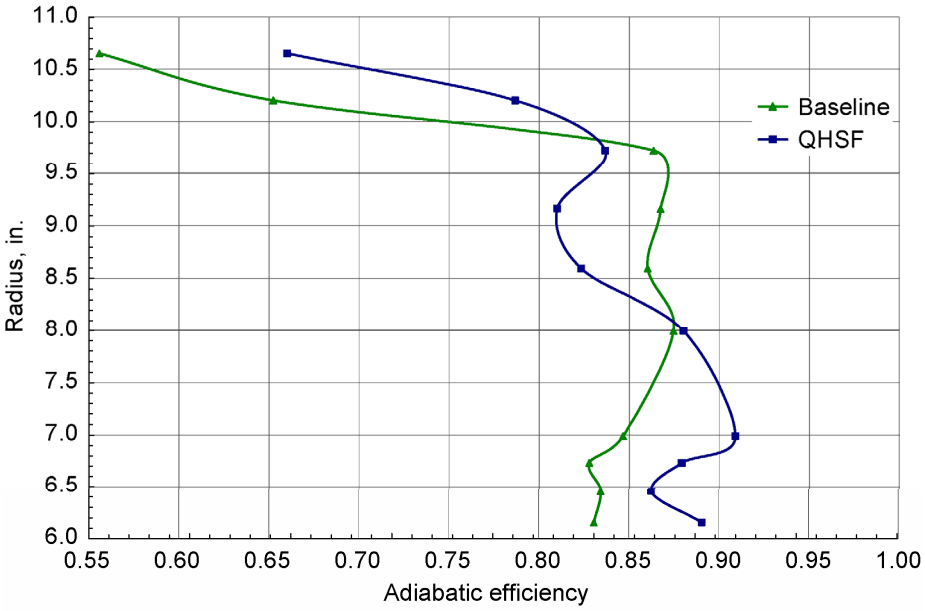

Figure 34.—Adiabatic efficiency profiles, 81% RPMc.

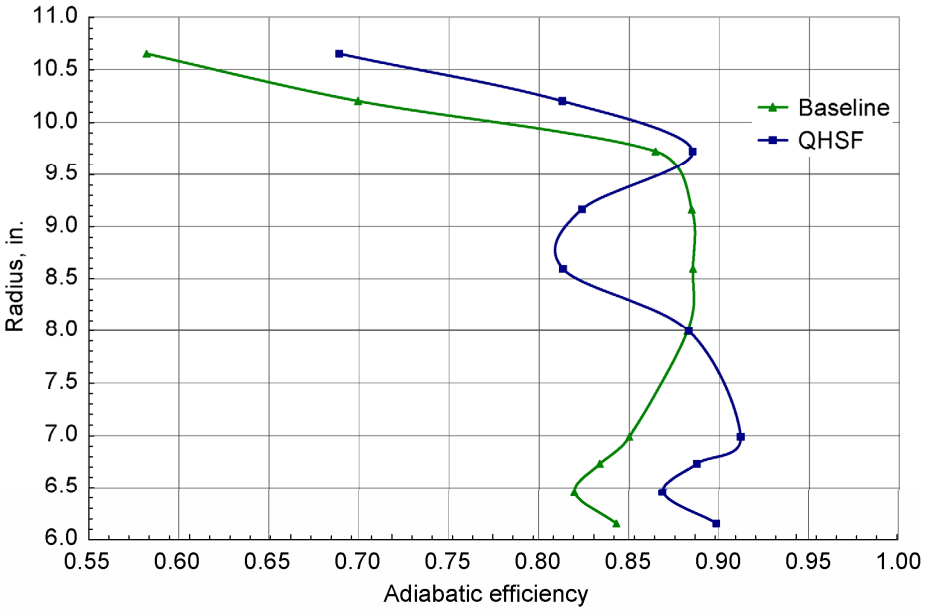

Figure 35.—Adiabatic efficiency profiles, 90% RPMc.

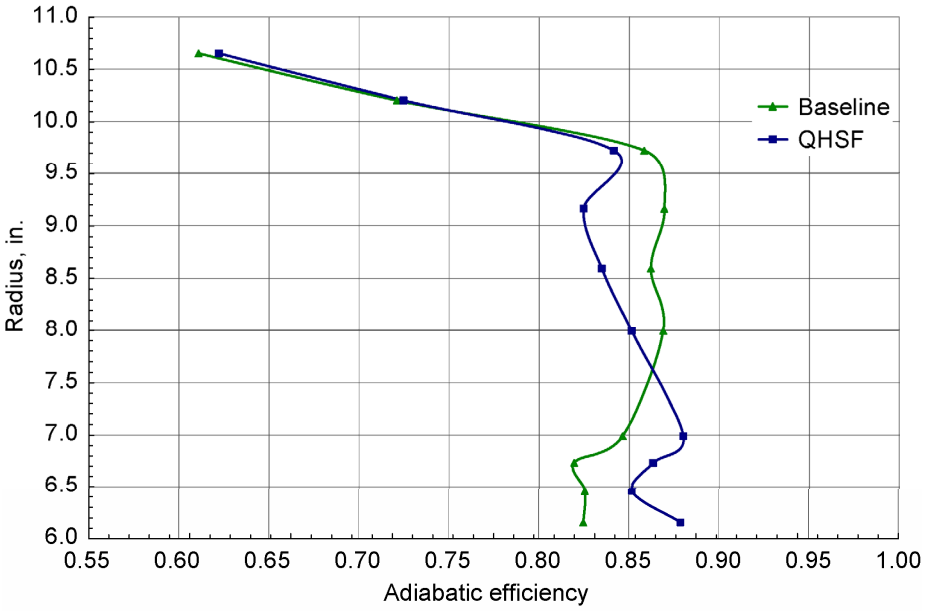

Figure 36.—Adiabatic efficiency profiles, 100% RPMc.

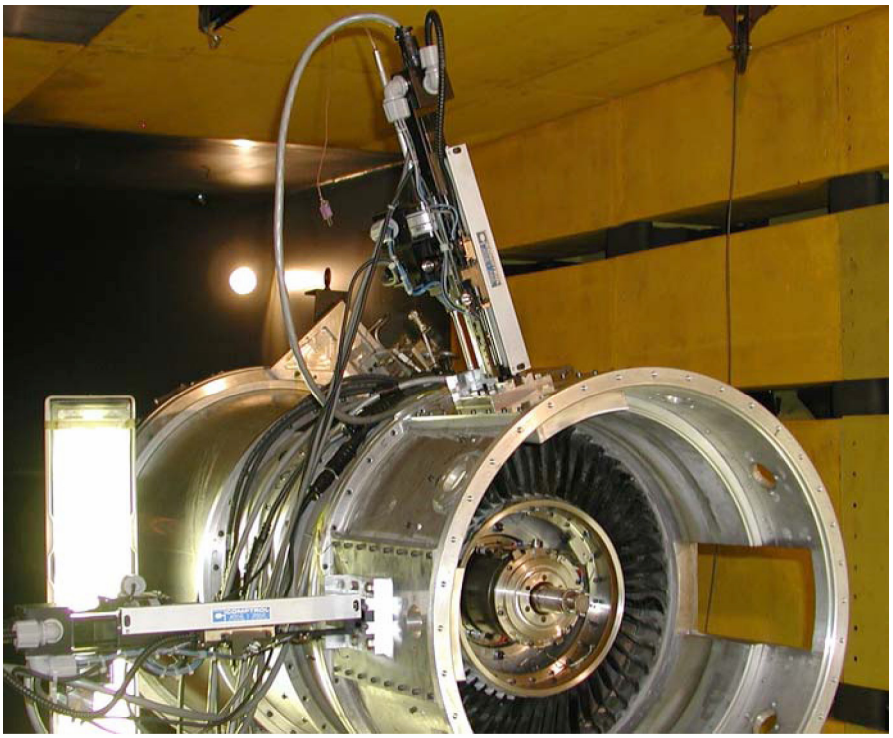

Figure 37.—Survey probe installation during model build-up.

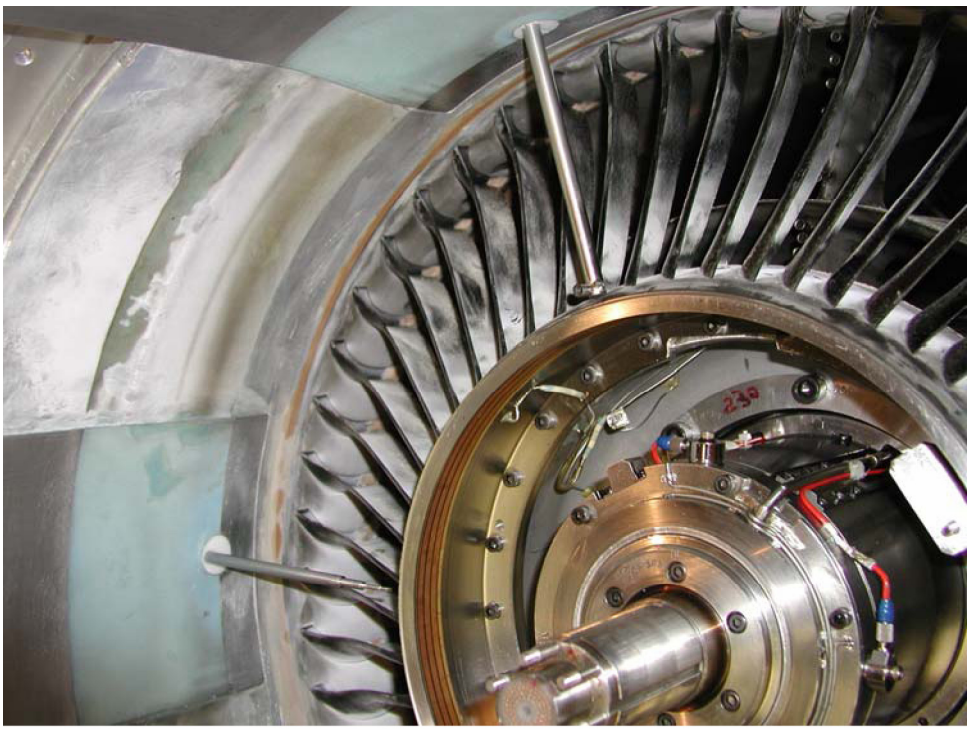

Figure 38.—Combo probe (top) and wedge probe (left) mounted in the model.

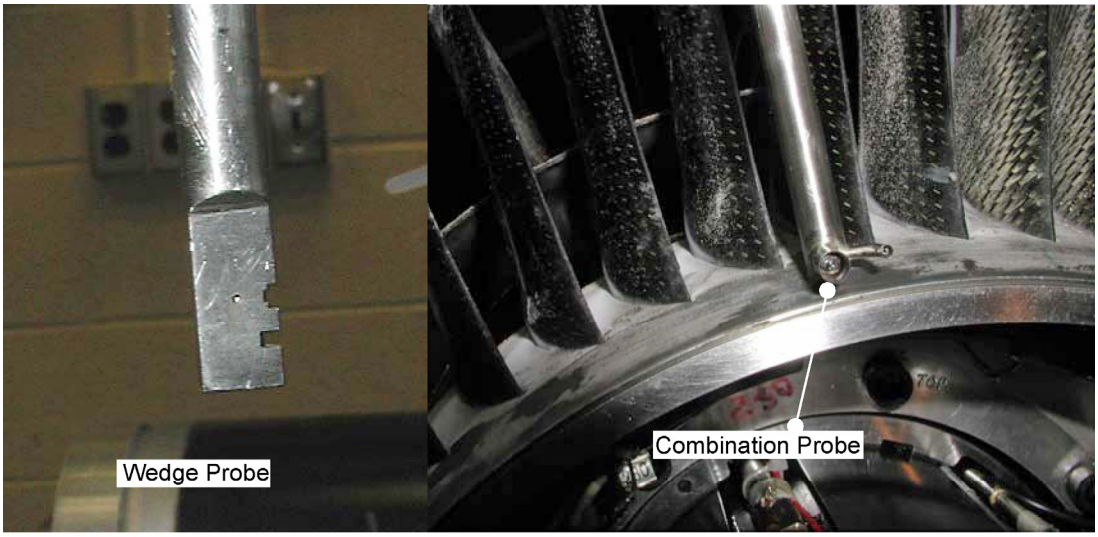

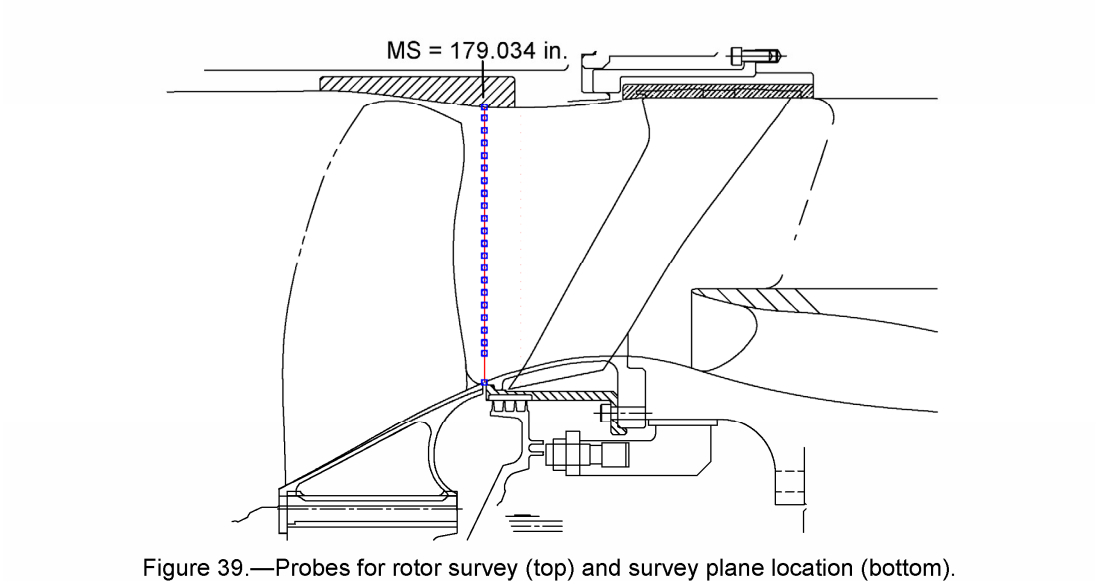

Figure 39.—Probes for rotor survey (top) and survey plane location (bottom).

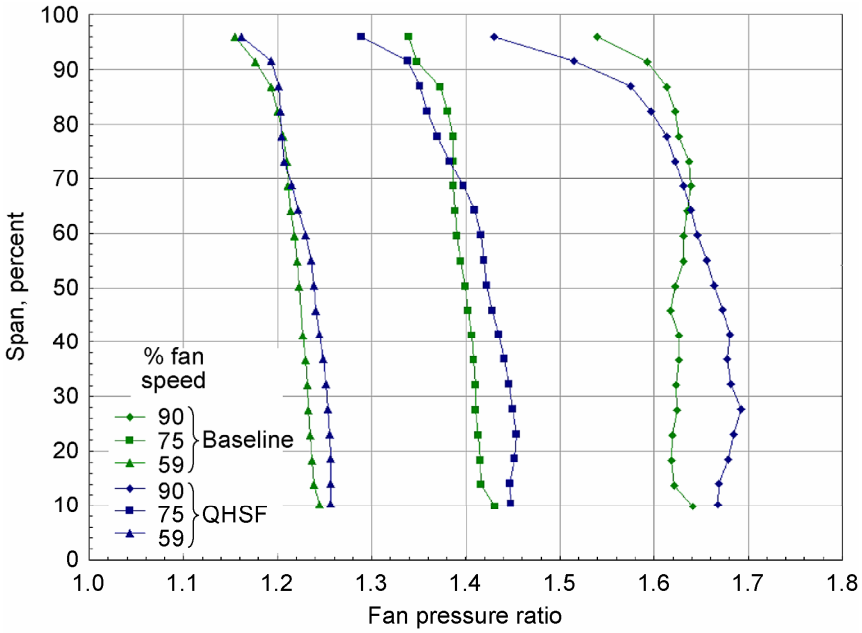

Figure 40.—Rotor pressure profile comparison, rotor survey data.

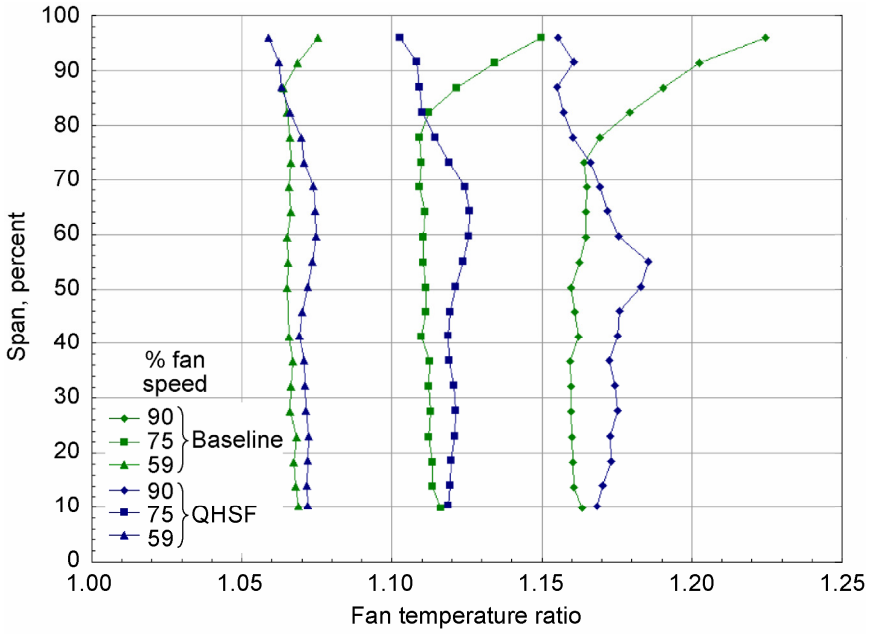

Figure 41.—Rotor temperature profile comparison, rotor survey data.

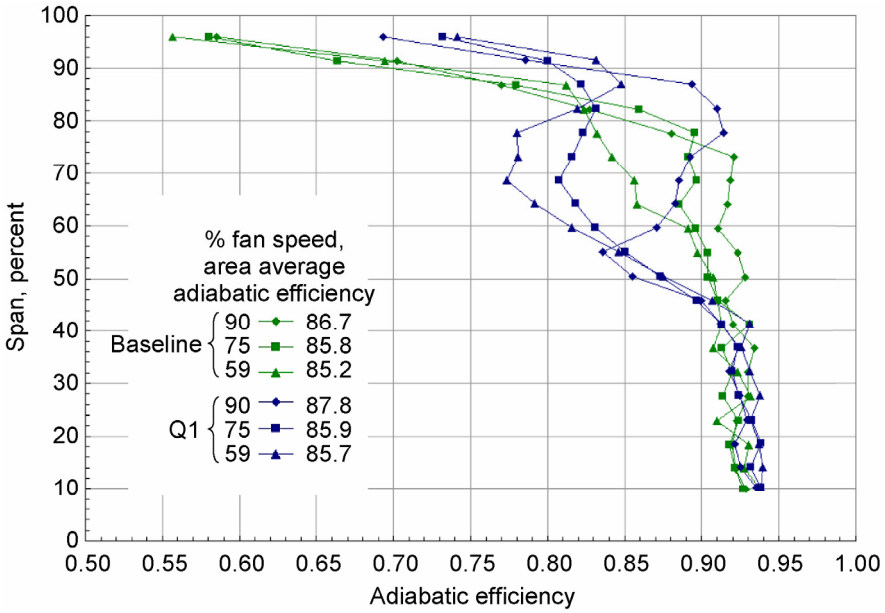

Figure 42.—Rotor efficiency comparison, rotor survey data.

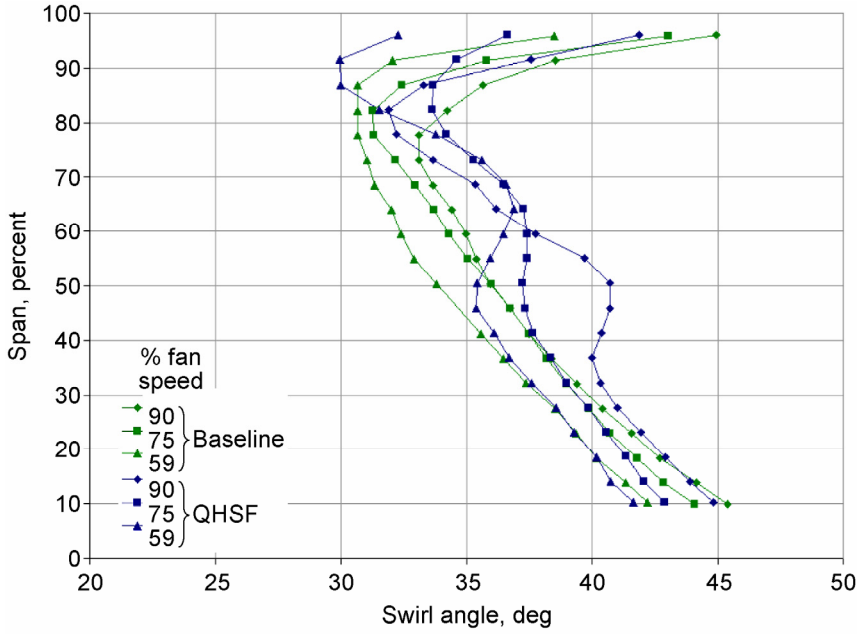

Figure 43.—Rotor swirl angle comparison, rotor survey data.

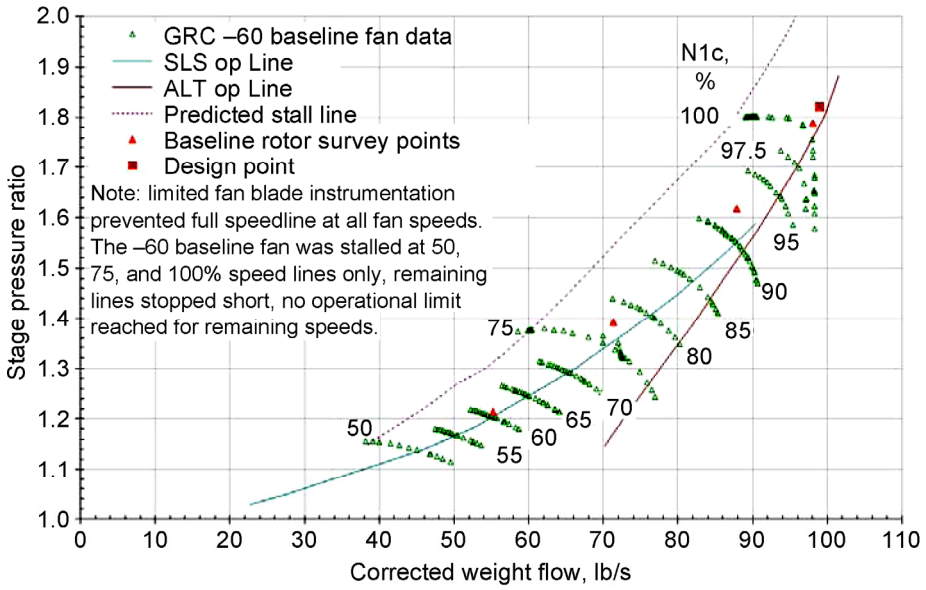

Figure 44.—Baseline map with stage and rotor data.

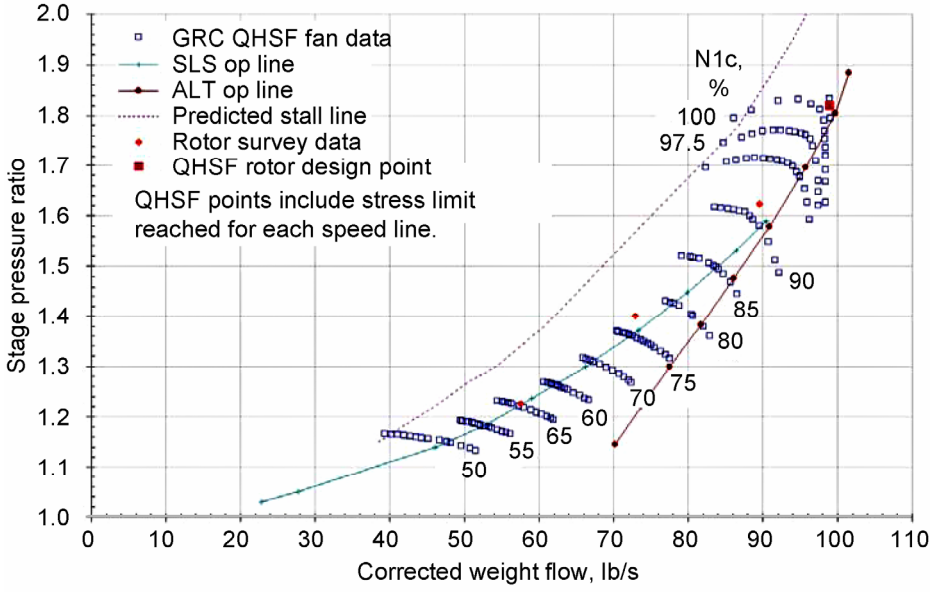

Figure 45.—QHSF map with stage and rotor data.

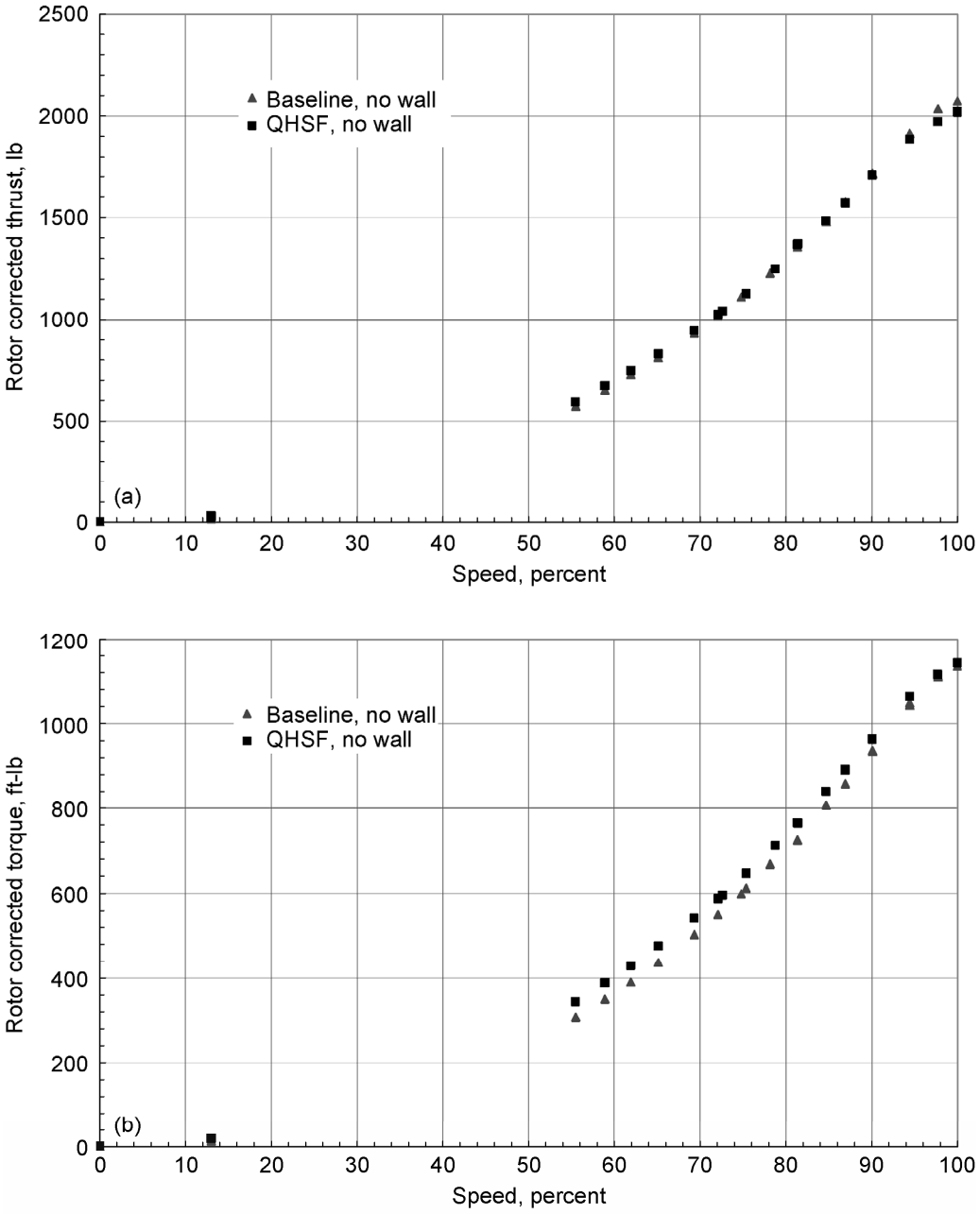

Figure 46.—Rotor thrust and torque versus percent speed. (a) Rotor thrust comparison baseline and QHSF. (b) Rotor torque comparison baseline and QHSF.

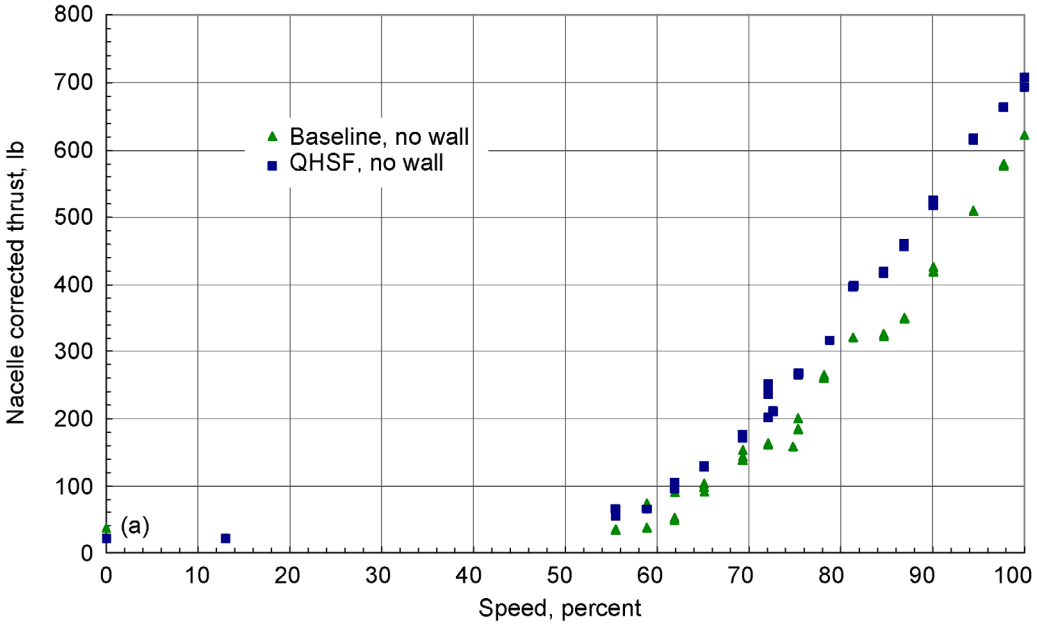

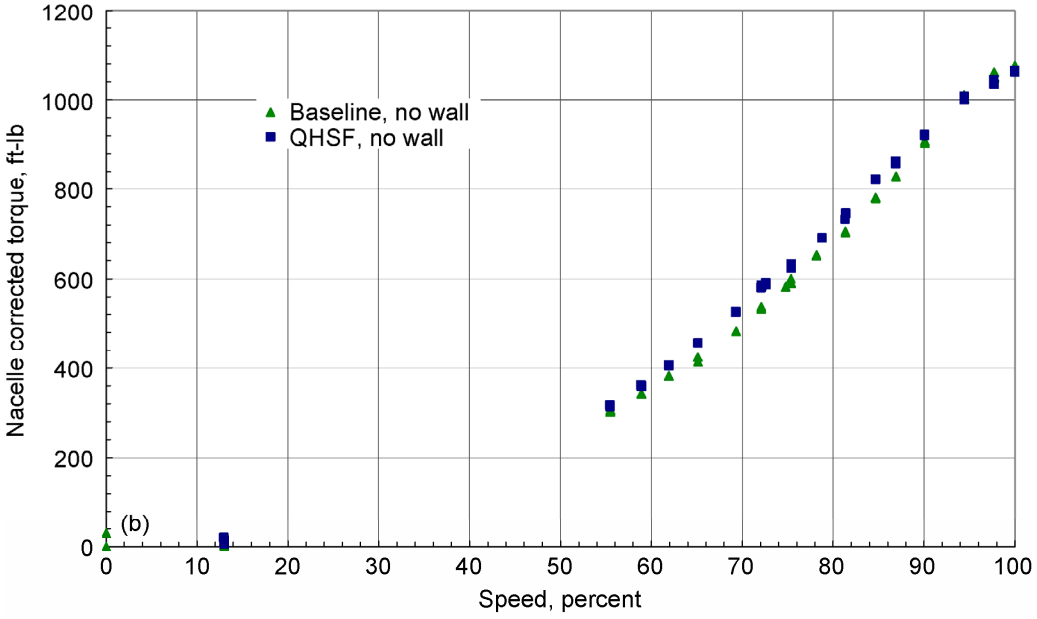

Figure 47.—Nacelle thrust and torque versus percent speed. (a) Nacelle thrust comparison baseline and QHSF. (b) Nacelle torque comparison baseline and QHSF.

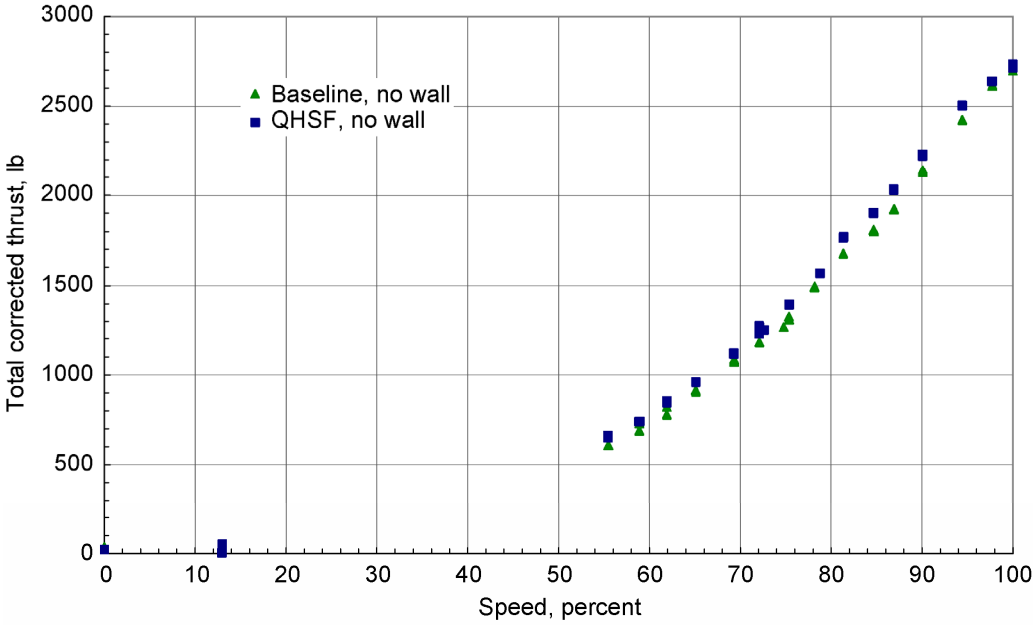

Figure 48.—Total thrust (fan plus FEGV) versus percent speed.

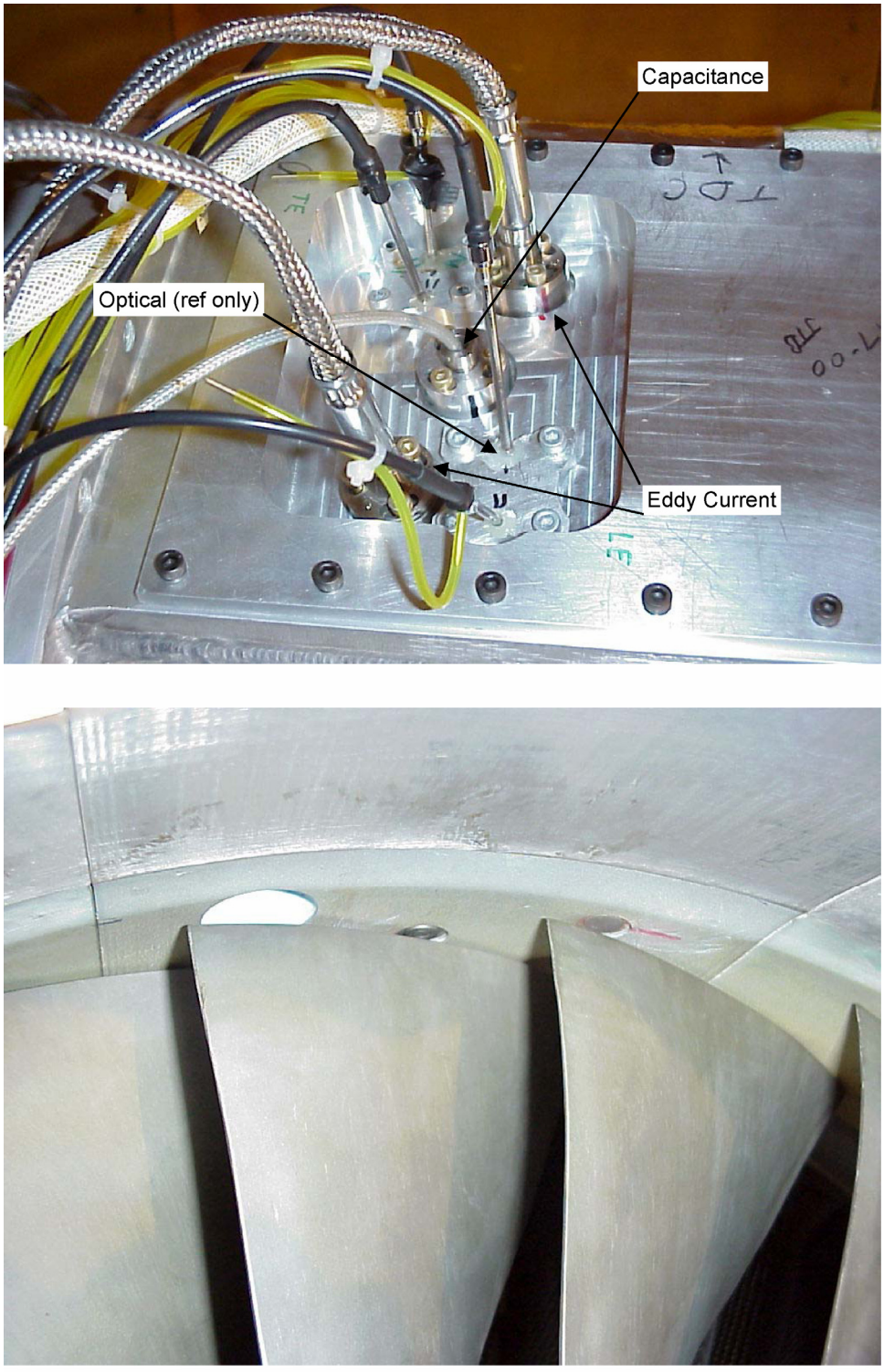

Figure 49.—Tip clearance probe installation.

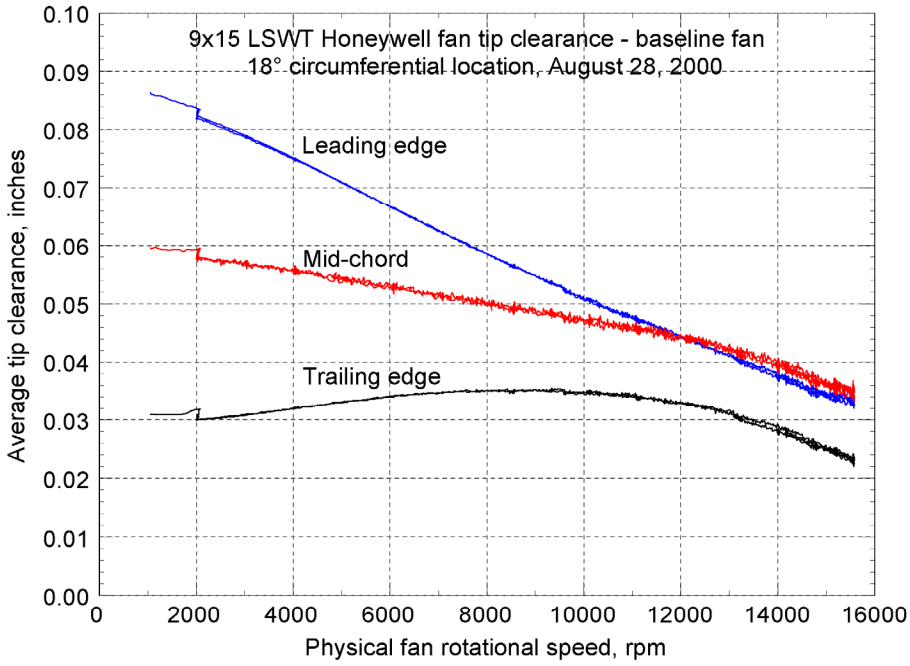

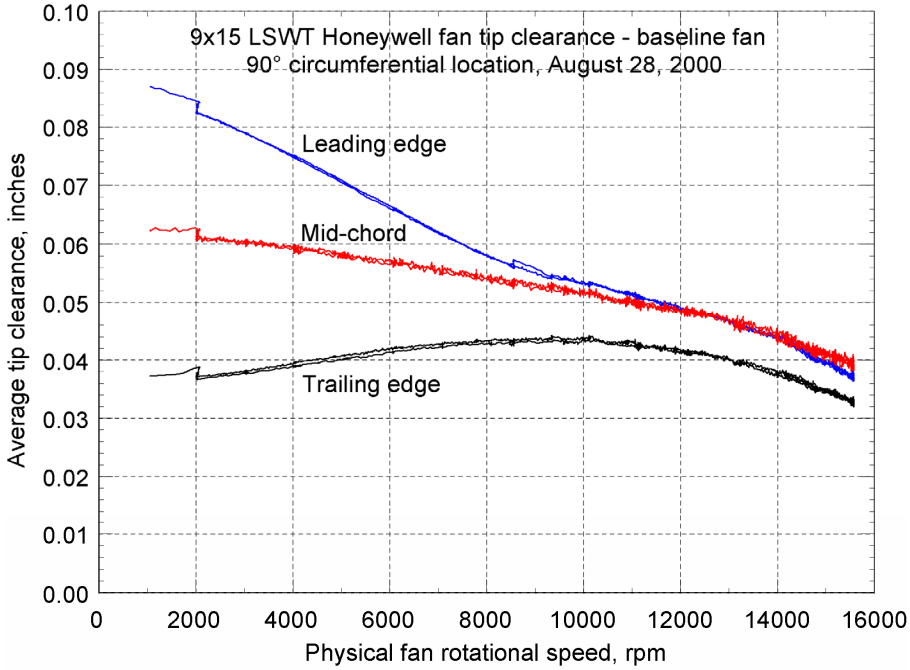

Figure 50.—Baseline tip clearance measurements.

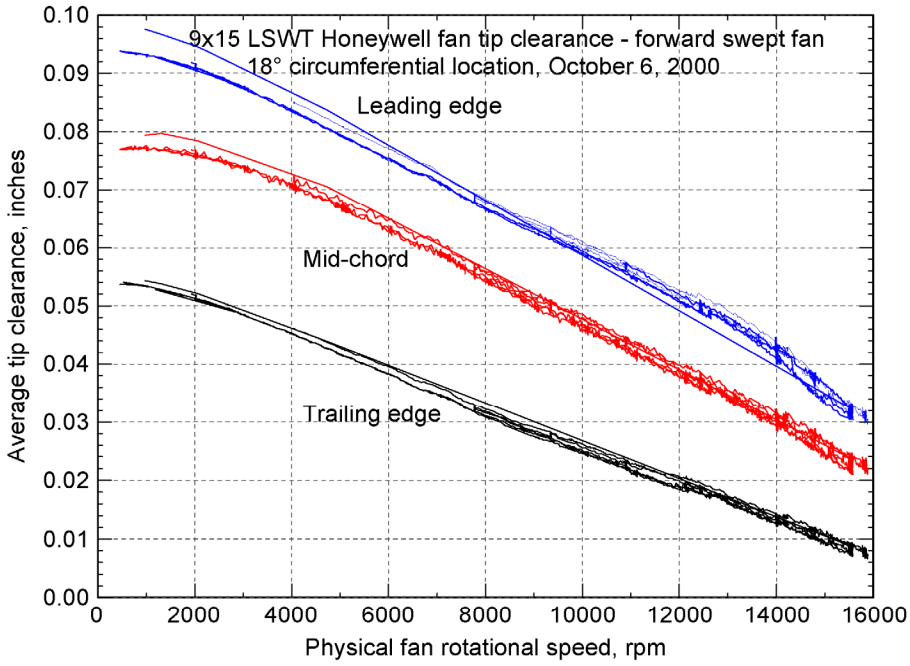

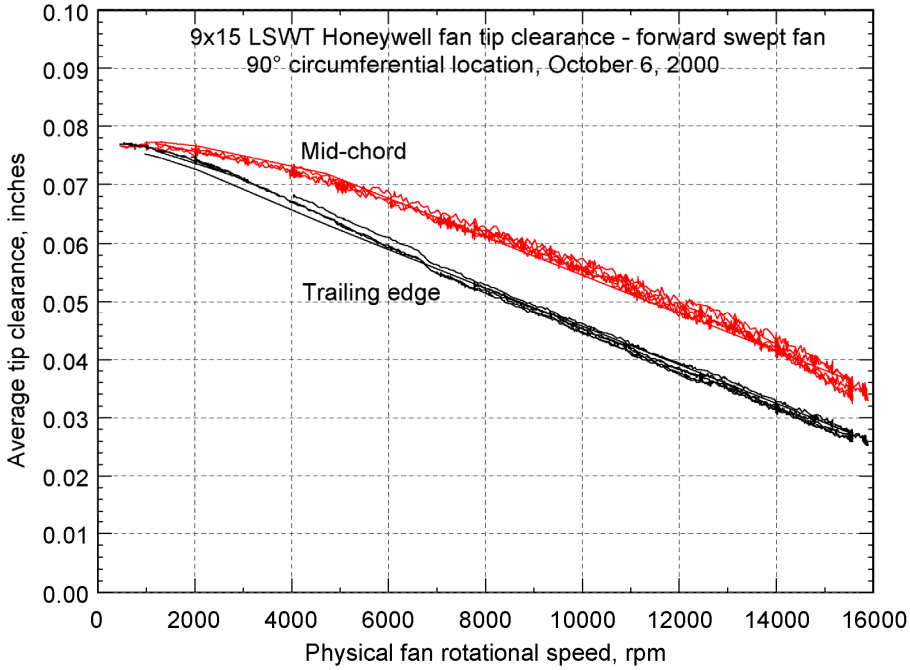

Figure 51.—QHSF tip clearance measurements.

REPORT DOCUMENTATION PAGE

Form Approved
OMB No. 0704-0188

1. AGENCY USE ONLY (*Leave blank*)	2. REPORT DATE	3. REPORT TYPE AND DATES COVERED
	December 2006	Technical Memorandum

4. TITLE AND SUBTITLE

Aerodynamic Performance Measurements for a Forward Swept Low Noise Fan

5. FUNDING NUMBERS

WBS–22–781–30–41

6. AUTHOR(S)

E. Brian Fite

7. PERFORMING ORGANIZATION NAME(S) AND ADDRESS(ES)

National Aeronautics and Space Administration
John H. Glenn Research Center at Lewis Field
Cleveland, Ohio 44135–3191

8. PERFORMING ORGANIZATION REPORT NUMBER

E–15693

9. SPONSORING/MONITORING AGENCY NAME(S) AND ADDRESS(ES)

National Aeronautics and Space Administration
Washington, DC 20546–0001

10. SPONSORING/MONITORING AGENCY REPORT NUMBER

NASA TM—2006-214413

11. SUPPLEMENTARY NOTES

Responsible person, E. Brain Fite, organization code RTA, 216–433–3892.

12a. DISTRIBUTION/AVAILABILITY STATEMENT

Unclassified - Unlimited
Subject Category: 02

Available electronically at http://gltrs.grc.nasa.gov

This publication is available from the NASA Center for AeroSpace Information, 301–621–0390.

12b. DISTRIBUTION CODE

13. ABSTRACT ***(Maximum 200 words)***

One source of noise in high tip speed turbofan engines, caused by shocks, is called multiple pure tone noise (MPT's). A new fan, called the Quiet High Speed Fan (QHSF), showed reduced noise over the part speed operating range, which includes MPT's. The QHSF showed improved performance in most respects relative to a baseline fan; however, a part-speed instability discovered during testing reduced the operating range below acceptable limits. The measured QHSF adiabatic efficiency on the fixed nozzle acoustic operating line was 85.1 percent and the baseline fan 82.9 percent, a 2.2 percent improvement. The operating line pressure rise at design point rotational speed and mass flow was 1.764 and 1.755 for the QHSF and baseline fan, respectively. Weight flow at design point speed was 98.28 lbm/sec for the QHSF and 97.97 lbm/sec for the baseline fan. The operability margin for the QHSF approached 0 percent at the 75 percent speed operating condition. The baseline fan maintained sufficient margin throughout the operating range as expected. Based on the stage aerodynamic measurements, this concept shows promise for improved performance over current technology if the operability limitations can be solved.

14. SUBJECT TERMS

Propulsive efficiency; Leading edge sweep; Turbofans; Ducted fan engines; Fan blades; Fans

15. NUMBER OF PAGES

48

16. PRICE CODE

17. SECURITY CLASSIFICATION OF REPORT	18. SECURITY CLASSIFICATION OF THIS PAGE	19. SECURITY CLASSIFICATION OF ABSTRACT	20. LIMITATION OF ABSTRACT
Unclassified	Unclassified	Unclassified	